WARWICK
THE UNIVERSITY OF WARWICK

Manuscript version: Author's Accepted Manuscript
The version presented in WRAP is the author's accepted manuscript and may differ from the published version or Version of Record.

Persistent WRAP URL:
http://wrap.warwick.ac.uk/168308

How to cite:
Please refer to published version for the most recent bibliographic citation information. If a published version is known of, the repository item page linked to above, will contain details on accessing it.

Copyright and reuse:
The Warwick Research Archive Portal (WRAP) makes this work by researchers of the University of Warwick available open access under the following conditions.

© 2022 Elsevier. Licensed under the Creative Commons Attribution-NonCommercial-NoDerivatives 4.0 International http://creativecommons.org/licenses/by-nc-nd/4.0/.

Publisher's statement:
Please refer to the repository item page, publisher's statement section, for further information.

For more information, please contact the WRAP Team at: wrap@warwick.ac.uk.

warwick.ac.uk/lib-publications

Title: Stochastic modelling of African swine fever in wild boar and domestic pigs: epidemic forecasting and comparison of disease management strategies

Author names and affiliations: Emmanuelle A. Dankwa [a], Sébastien Lambert [b,1], Sarah Hayes [c], Robin N. Thompson [d, e], Christl A. Donnelly [a, c*]

[a] Department of Statistics, University of Oxford, Oxford, United Kingdom

[b] Centre for Emerging, Endemic and Exotic Diseases, Department of Pathobiology and Population Sciences, Royal Veterinary College, University of London, United Kingdom

[c] Department of Infectious Disease Epidemiology, Faculty of Medicine, School of Public Health, Imperial College London, United Kingdom

[d] Mathematics Institute, University of Warwick, Coventry, United Kingdom

[e] Zeeman Institute for Systems Biology and Infectious Disease Epidemiology Research, University of Warwick, Coventry, United Kingdom

[1] Present address: IHAP, Université de Toulouse, INRAE, ENVT, Toulouse, France

***Corresponding author:** Christl A. Donnelly, Department of Statistics, University of Oxford, 24-29 St Giles', Oxford OX1 3LB, United Kingdom

Email address: christl.donnelly@stats.ox.ac.uk

Abstract: African swine fever (ASF), caused by the African swine fever virus (ASFV), is highly virulent in domestic pigs and wild boar (*Sus scrofa*), causing up to 100% mortality. The recent epidemic of ASF in Europe has had a serious economic impact and poses a threat to global food security. Unfortunately, there is no effective treatment or vaccine against ASFV, limiting the available disease management strategies. Mathematical models allow us to further our understanding of infectious disease dynamics and evaluate the efficacy of disease management strategies. The ASF Challenge, organised by the French National Research Institute for Agriculture, Food, and the Environment, aimed to expand the development of ASF transmission models to inform policy makers in a timely manner. Here, we present the model and associated projections produced by our team during the challenge. We developed a stochastic model combining transmission between wild boar and domestic pigs, which was calibrated to synthetic data corresponding to different phases describing the epidemic progression. The model was then used to produce forward projections describing the likely temporal evolution of the epidemic under various disease management scenarios. Despite the interventions implemented, long-term projections forecasted persistence of ASFV in wild boar, and hence repeated outbreaks in domestic pigs. A key finding was that it is important to consider the timescale over which different measures are evaluated: interventions that have only limited effectiveness in the short term may yield substantial long-term benefits. Our model has several limitations, partly because it was developed in real-time. Nonetheless, it can inform understanding of the likely development of ASF epidemics and the efficacy of disease management strategies, should the virus continue its spread in Europe.

Keywords (5 max.): mathematical modelling; African swine fever virus; wildlife-livestock interface; spatial model; real-time analysis

1 Introduction

1.1 Background to African Swine Fever

African swine fever (ASF) is a highly contagious viral disease capable of infecting all swine. It is caused by the African swine fever virus (ASFV), a double-stranded DNA virus that is the sole member of the Asfarviridae family. ASFV is endemic across much of sub-Saharan Africa (Penrith et al., 2019). An ancient sylvatic cycle involving warthogs (*Phacochoerus africanus*) and soft ticks of the species *Ornithodoros* exists in eastern and southern Africa (Chenais et al., 2018; Costard et al., 2013; Dixon et al., 2019; Penrith et al., 2019). Juvenile warthogs are infected with the virus within the first few weeks of their lives when they are bitten by ticks living within their burrows. They develop a transient viraemia and remain infected for life but do not show any clinical signs of disease (Jori et al., 2013). The situation is very different in domestic pigs and wild boar (*Sus scrofa*) in which ASFV causes a range of clinical signs including sudden death, haemorrhage, lethargy, high fever and inapparent infection (Blome et al., 2020, 2013). Mortality rates range between 0-100% depending on the strain of the virus, the host, the viral dose, and the route of exposure (Blome et al., 2013, 2012; Costard et al., 2013). The existence of a carrier state following recovery from lower virulence strains has been suggested (Dixon et al., 2019).

Transmission routes for ASFV include direct contact between swine, contact with infected carcasses, meat products, fomites, the environment, and tick vectors (Costard et al., 2013; Guinat et al., 2016a; Pepin et al., 2020). A transmission cycle involving haematophagous flies has been suggested to occur in Europe, but its importance is still uncertain (Mellor et al., 1987; Olesen et al., 2018; Vergne et al., 2021). Transmission between wild boar and domestic pigs has been demonstrated (Dixon et al., 2019; Guinat et al., 2016a) and is thought to play an important role in the spread of ASFV. In high-biosecurity commercial pig farms where contact with wild boar has been excluded as a means of transmission, indirect transmission mediated by humans is usually considered the most likely route of introduction (Guinat et al., 2016a; Olesen et al., 2018). Infected animal carcasses have also been identified as a potential route of transmission and under certain conditions could pose a risk of infection for several months

(Fischer et al., 2020). Wild boar have been shown to have frequent contact with conspecific carcasses (Probst et al., 2017) and carcass-based transmission may be especially important in locations with low host density (Pepin et al., 2020).

The strains currently circulating in Europe have shown high virulence during experimental infection of domestic pigs and wild boar (Blome et al., 2020). Typically, death occurs within 7-10 days post-infection, but survival up to 36 days post-infection has been reported (Blome et al., 2020; Pietschmann et al., 2015). There is currently no approved treatment or vaccine against ASFV. Instead, disease management measures include culling on infected pig farms, disinfecting farm equipment, imposing restrictions on pork trade, conducting epidemiological surveillance of domestic pig and wild boar populations and managing wild boar populations (World Organisation for Animal Health, 2021).

1.2 Current situation in Europe

Although ASFV was eradicated from most of Europe in the 1990s (with the exclusion of Sardinia, where ASFV genotype I remains endemic to date), it was reintroduced to the continent via Georgia in 2007, most likely by importation of infected pork products (Beltrán-Alcrudo et al., 2008; Rowlands et al., 2008). Following its introduction, ASFV became established in the local wild boar population leading to further outbreaks in domestic pigs, with transmission between infected wild boar and domestic pigs thought to play an important role in the spread of the disease (Dixon et al., 2019; Gogin et al., 2013; Oganesyan et al., 2013). In 2014, the first cases were reported in the European Union (EU) (European Food Safety Authority, 2015). Since then, a series of outbreaks have been recorded resulting in major economic losses for the European pig industry (Danzetta et al., 2020; Guinat et al., 2016a). EU countries that have been affected by the current ASFV strain (genotype II) include Belgium, Bulgaria, Czech Republic, Estonia, Germany, Greece, Hungary, mainland Italy, Latvia, Lithuania, Poland, Romania, Serbia, and Slovakia (Blome et al., 2020). The first ASFV cases in Germany were reported in wild boar in September 2020 (Sauter-Louis et al., 2021a). Then, in July 2021, ASFV was confirmed in two domestic pig herds in the Brandenburg region

bordering Poland (International Society for Infectious Diseases, 2021). Most recently, in January 2022, ASFV genotype II was confirmed in wild boar in mainland Italy (International Society for Infectious Diseases, 2022). Belgium and the Czech Republic are the only EU countries that have successfully eradicated ASFV following its introduction during the current epidemic. Outbreaks in these two countries were geographically localised and confined to the wild boar population. Disease management measures implemented included fencing off high-risk areas to limit movement of wild boar, active search and removal of wild boar carcasses and alterations to hunting patterns (Dellicour et al., 2020; Marcon et al., 2020). Whilst ASFV was eradicated from most of Europe in the 1990s, it has remained endemic in Sardinia since its introduction in 1978. The epidemiology of ASFV in Sardinia is complicated by the presence of free-roaming domestic pigs (FRPs) which have hindered previous eradication efforts. However, recent evidence highlighting the central role that FRPs play in maintaining ASFV and the implementation of a new eradication programme have led to marked reductions in the levels of ASFV in Sardinia and eradication appears achievable if the controls are maintained (Viltrop et al., 2021).

Whilst we focus on the situation in Europe here, it is worth noting that ASFV continues to circulate across sub-Saharan Africa (Mulumba-Mfumu et al., 2019; World Organisation for Animal Health, 2020) and, since its introduction to Asia in 2018, ASFV has spread to many Asian countries causing substantial economic impacts and posing a threat to vulnerable and endangered wild pig species (Luskin et al., 2020; Mighell and Ward, 2021; Tian and von Cramon-Taubadel, 2020). In 2021, ASFV was reported in the Americas for the first time in almost 40 years when the disease was reported in the Dominican Republic in July 2021 and then in Haiti in September 2021 (Gonzales et al., 2021; U.S. Department of Agriculture, 2021; World Organisation for Animal Health, 2022).

1.3 Mathematical models

The first mathematical models of ASFV were published in 2011 following introduction of the virus to Europe (Hayes et al., 2021). Since then, mathematical models have been widely utilised to further our understanding of the transmission dynamics of ASFV (see Hayes et al. (2021) for a recent review). Examples of the uses of modelling studies of ASFV include estimation of epidemiological parameters (Barongo et al., 2015; de Carvalho Ferreira et al., 2013; Guinat et al., 2018, 2016b; Gulenkin et al., 2011; Hu et al., 2017; Lange and Thulke, 2017; Loi et al., 2020; Nielsen et al., 2017; Pietschmann et al., 2015; Shi et al., 2020), investigation of transmission dynamics in particular species (Halasa et al., 2019, 2016a; Mur et al., 2018; O'Neill et al., 2020; Pepin et al., 2021, 2020; Taylor et al., 2021), exploration of the role of vectors in transmission (Vergne et al., 2021) and assessment of the potential impacts of interventions (Barongo et al., 2016; Croft et al., 2020; Gervasi et al., 2020; Halasa et al., 2016b; Lange, 2015; Lange et al., 2018; Lange and Thulke, 2015; Lee et al., 2021; Taylor et al., 2021; Thulke and Lange, 2017).

Single-species models are used most frequently, despite the important role of between-species transmission of ASFV (Taylor et al., 2021). Domestic pig models may incorporate within-herd and/or between-herd transmission whilst wild boar models are frequently individual-based spatially structured models that incorporate existing knowledge of wild boar demography. Many models of ASFV transmission use the classic Susceptible-Exposed-Infectious-Removed (SEIR) structure (Guinat et al., 2018; Halasa et al., 2019), with some including an extra class for infectious/non-infectious carcasses (Pepin et al., 2021). Other variations include using a Susceptible-Latent-Subclinical-Clinical-Removed structure (Halasa et al., 2016a), in which the infectious stage is split into sub-clinical and clinical stages, and a Susceptible-Infectious-Carrier-Removed structure (O'Neill et al., 2020) which incorporates the possibility that pigs that have recovered from lower virulence strains continue to carry the virus.

1.4 Challenge overview and objectives

Motivated by the ongoing global spread of ASFV, the French National Research Institute for Agriculture, Food and the Environment (INRAE) organised the ASF Challenge to expand the development and application of mathematical methods for ASF epidemic forecasting and to better understand the strengths and limitations of different modelling approaches (Picault et al., 2021). An additional goal was to improve the readiness of modelling teams and hence their ability to advise policy makers in a timely manner when faced with emerging epidemic threats such as ASF (https://www6.inrae.fr/asfchallenge/). Similar events in the past have led to important statistical and computational innovations for epidemic forecasting and have fostered fruitful collaborations between research teams and policy makers (Johansson et al., 2019; McGowan et al., 2019; Viboud et al., 2018).

The challenge took place from August 2020 to January 2021. It was comprised of three phases, describing different stages of a simulated ASF epidemic on a fictional island (Merry Island). In each phase, simulated data regarding the number and location of reported infected pig herds and wild boar – as well as simulated data describing movements of pigs exchanged or traded between herds – were provided. Modelling teams were then asked to provide projections, informed by their own analyses, of the course of the epidemic over a specified future time period (generally 30 days) incorporating specified disease management measures where indicated. Day 0 represented the date of the first reported case of ASF on Merry Island. In phase 1, simulated data from days 0 to 50 (period 1) were provided, with projections requested for days 51 to 80 (period 2). In phase 2, simulated data from periods 1 and 2 were provided to underpin projections for days 81 to 110 (period 3). Finally, in phase 3, simulated data were provided from days 0 to 110 with two sets of projections requested: one short-term set for days 111 to 140 and one longer-term set for days 111 to 230.

Here we provide details of the model and the associated projections that were produced by our team in each phase of the challenge. To facilitate reproducibility, we have made all code and relevant data files used for this analysis freely available on GitHub: https://github.com/emmanuelle-dankwa/ASF_model.

2 Materials and methods

2.1 Synthetic data provided by the challenge coordinators

2.1.1 Demographic data

In the challenge, a simulated ASF epidemic on Merry Island – a fictional island located in the North Atlantic Ocean with area 144,208 km^2 divided into 25 administrative units – was considered. There were 4,532 registered pig farms on the island. Farms were classified as either backyard or commercial, and either outdoor or indoor. For each farm, additional information provided included the size of the pig herd, its geographical coordinates, its production type (farrow-to-wean, farrow-to-finish or finishing), and whether it belonged to the same producer as other farms (i.e., “multisite farms” comprising several geographically distinct farms). Farms belonging to the same producer were expected to be more epidemiologically connected to each other than to any other farm. Outdoor herds were assumed to be in contact with the wild boar population (see Model section). There were 1069 registered outdoor herds (23.6%), scattered throughout the Island (see Figure A1, Appendix A).

In addition to these registered farms, there was an unknown number of small, unregistered farms. Eight unregistered farms were identified in total from period 1 to 3 and were added to the 4,532 registered farms: two farms were identified because they became infected, four farms were identified because they became part of a surveillance zone, and two others were identified because they were culled preventively.

Registered movements of pigs in the trade network were provided for the two months before the first detected infected pig herd (suspected on 8th July 2020, referred to as “day 0” during the challenge, and confirmed three days later), with the day at which each movement occurred, the source and destination herds, and the number of pigs traded.

Finally, data on the hunting bag (number of boar hunted during a hunting season) in each administrative unit in 2019 (the calendar year before the detection of ASFV) were also provided (260,675 hunted wild boar in total). It was estimated by the ASF Challenge coordinators that around 50% of wild boar are shot during a hunting season, giving a rough wild boar population size estimate of 521,350 for Merry Island.

2.1.2 Epidemiological data

In each of the three phases of the challenge, incidence data for both pigs and wild boar were provided. This synthetic epidemiological data originated from an epidemiological model developed by the challenge coordinators, which remained unknown to the participating teams at the time of the challenge. Briefly, the model used to produce synthetic epidemiological data was a discrete-time, stochastic, spatially explicit and agent-based model. Agents were pig herds and individual wild boar, each with their specific location. Transmission pathways included transmission between wild boar, transmission between pig herds (via introduction of infected pigs through trade movements or indirect contact with infectious farms), and transmission from wild boar to pig herds and vice versa. Trade movements were determined based on a temporal directed graph between farms. All other transmission pathways were modelled based on an exponential transmission kernel, assuming that the contribution of infected pig farms was proportional to their within-herd prevalence (modelled using a within-herd compartmental SEIRD – Susceptible, Exposed, Infectious, Recovered, Deceased – model). The synthetic data corresponded to one stochastic simulation of the model. Further details on the original model and data generation can be found in the first article in this special issue (Picault et al., 2021).

For pig herds, the data provided included the identity of each herd in which infection was detected, with the mode of detection as well as the dates of suspicion, confirmation, and culling. The first reported infected herd was herd 3594, and two other infected herds were detected during period 1 (days 0 to 50). Nine new infected herds were confirmed during period 2 (days 51 to 80), followed by 14 others during period 3 (days 81 to 110), resulting in a total of 26 detected infected pig herds from period 1 to period 3 (days 0 to 110). For wild boar, the locations of tested wild boar found each day through passive surveillance, active surveillance and hunting were provided, as well as the date of confirmation and the test results (positive or negative). A total of 2,984 detected infected wild boar were reported from period 1 to period 3 (days 0 to 110). Although the epidemiological data provided were synthetic, we later refer to

them as “observed data” to clearly distinguish the results of our model from the data to which they were compared.

Contextual information on disease management measures in both pig herds and wild boar was also provided by the challenge coordinators in each phase (see details in Model section below).

2.2 Model

We modelled ASFV transmission on Merry Island using a model combining a stochastic, spatial Susceptible-Infectious-Post-infectious (SIP) model for transmission across the island via wild boar and a stochastic, metapopulation Susceptible-Exposed-Infectious-Recovered-Deceased (SEIRD) model for pig herds. The model included transmission from wild boar to pig herds but did not account for transmission from pig herds to wild boar since we saw no evidence, based on the synthetic data provided by the challenge coordinators, of such transmission. All simulations and analyses were performed with R version 4.0.5 (R Core Team, 2022).

2.2.1 Transmission

2.2.1.1 Wild boar

Transmission via wild boar was modelled using a stochastic SIP model with an exponential spatial dispersal kernel. Due to the large number of wild boar on the island and for computational efficiency, only wild boar within a defined area around the initial detected cases in wild boar and pig herds were considered (see Appendix A for details). Wild boar live in matrilineal groups, with reported mean group sizes of 4-8 individuals (Maselli et al., 2014; Pepin et al., 2020; Podgórski et al., 2014). These groups are typically composed of adult and subadult females and their offspring (Pepin et al., 2020). Reports of home range sizes vary but are typically estimated as between 2–10 km^2 (Janeau et al., 1995; Keuling et al., 2008; Podgórski et al., 2013). To represent this social structure, we divided the area into 2500 rectangular patches and assumed that the infectious pressure on every susceptible wild boar

within a specific patch was identical. Thus, patches were treated as model units. The area per patch was 16 km^2 in phase 1, and 7.5 km^2 in phases 2 and 3. Patch dimensions were reduced in the latter phases to enable a finer-grained resolution for more accurate results.

In addition to tracking the health states of patches, we also tracked the health state of each wild boar in a patch. Each day, a patch was either susceptible S, infectious I, or post-infectious P: a patch was considered infectious if at least one boar within the patch was infectious; a patch was considered susceptible if there were no infectious boar within the patch; and a patch was considered post-infectious if all boar in the patch were carcasses that were no longer infectious (see Appendix A, Table A1). We assumed that infected wild boar were infectious immediately after infection. As we assumed 100% mortality in wild boar for this strain of ASFV (Blome et al., 2013, 2012), the infectious wild boar transitioned to become a carcass after a fixed period of 14 days after infection (ASF modelling challenge coordinators, 2020; Hayes et al., 2021; Pietschmann et al., 2015) if it had not been removed (by hunting) before then. Although the period from infection to end of infectiousness (latent period) was set to 14 days, based on the upper limits of estimates for infection to infectiousness (4-5 days) and the duration of infectiousness (2-9 days), we also conducted a sensitivity analysis in which we explored different lengths of the latent period. Carcasses remained infectious for 90 days after death (ASF modelling challenge coordinators, 2020; Fischer et al., 2020) if not removed by surveillance before then. Thus, a carcass could either be in the I or P state, depending on whether the boar died less than/more than 90 days ago. Carcasses could not be re-infected.

For each patch, the number of new infections at each daily time step was chosen stochastically assuming a Poisson distribution with rate equal to the total “infectious pressure” being exerted on the patch. The infectious pressure on a patch j (accounting for the number of susceptible boar in patch j that are available for infection) exerted by an infected patch i at day t was given by

$$\beta_{ij}(t) = \beta \exp\left(\frac{-d_{ij}}{\alpha}\right) I_i(t) S_j(t) \tag{21}$$

where $\beta > 0$ determines the overall infection rate, $\alpha > 0$ is the scale parameter of the exponential dispersal kernel, $\exp(.)$, d_{ij} is the Euclidean distance between the midpoints of patches i and j (measured in km), $I_i(t)$is the number of infected wild boar in patch i on day t and $S_j(t)$ is the number of susceptible wild boar in patch j on day t. The total infectious pressure on patch j at day t, $\omega_j(t)$, was computed as the sum of the infectious pressures exerted on j:

$$\omega_j(t) = \sum_i \beta_{ij}(t) \tag{22}$$

The number of new infections in boar in each patch was determined by treating the infectious pressures as Poisson rates:

$$n_j \sim \mathrm{Pois}(\omega_j) \tag{23}$$

where n_j is the number of new infections in patch j. The specific wild boar infected in each patch on any day were randomly selected from the remaining susceptible boar in the patch. If n_j was greater than the number of susceptible wild boar remaining in the patch, all susceptible boar in the patch became infected.

2.2.1.2 Pig herds

The transmission model for pig herds considered individual pigs by describing the numbers of animals in each compartment within a herd, and the flows between the different compartments. Each herd was considered as a homogeneous, random-mixing population, not accounting for any within-herd structure (Guinat et al., 2018; Halasa et al., 2016a). Health statuses were susceptible S, exposed and pre-infectious E, infectious I, and immune (recovered) R. In addition, we distinguished infectious animals into subclinical (Isc) and clinical stages (Ic) (Halasa et al., 2016a).

The force of infection λ_i (equation (24)) exerted on susceptible pigs in herd i at time t was calculated based on: (1) the proportion of infectious pigs and of infectious residues from dead pigs within herd i (Fischer et al., 2020; Halasa et al., 2016a); (2) the local spread due, for

example, to shared material and fomites from neighbouring infected herds within a 2 km radius (Andraud et al., 2019; Halasa et al., 2016c); and (3) for outdoor herds, the number of infectious wild boar (alive and carcasses) in each infected patch and the distance between the herd and each infected patch using an exponential kernel:

$$\lambda_i(t) = 1 - \exp\left(-\beta^{PH} * \frac{I_i(t) + D_i(t)}{N_i(t)} - \sum_j \left(\frac{\rho}{d_{ij}} * \frac{I_j(t) + D_j(t)}{N_j(t)}\right) - \Omega_i(t)\right) \quad (24)$$

where $\beta^{PH} > 0$ is the transmission rate within pig herds (Table 51), $I_i(t)$ is the total number of infectious pigs in herd i (subclinical and clinical cases), $D_i(t)$ is the contribution of residues from dead pigs in herd i to transmission, $N_i(t)$ is the total number of live pigs in herd i, $\rho > 0$ is the transmission rate by local spread (Table 51), d_{ij} is the distance between herds i and j, and $\Omega_i \geq 0$ is the infectious pressure exerted by wild boar on outdoor herd i ($\Omega_i = 0$ for indoor herds).

Susceptible pigs S that acquired infection moved to the exposed pre-infectious compartment E, where they stayed during the pre-infectious period (with average duration δ), and then moved into the infectious compartment I, where they stayed during the infectious period (with average duration γ). Infectious pigs were first subclinical (Isc) during the subclinical period (average duration ϕ), and then became clinical (Ic) for the rest of the duration of the infectious period. Infectious pigs either survived and became immune and moved into the recovered compartment R, or died with probability μ (Halasa et al., 2016a). Although dead pig carcasses were assumed to be removed, dead pigs entered the compartment D to represent residues from dead animals contributing to transmission. These residues stayed in the environment during the mean lifetime of the virus in residues (with average duration τ). We assumed lifelong immunity in the R compartment. Parameter values are given in Table 51.

In addition to transmission by local spread, between-herd transmission was explicitly driven by the modelling of animal movements in the trade network (Brooks-Pollock et al., 2014), where animals in each compartment could enter or leave a herd, representing opportunities

of contacts and transmission between individuals from different herds (see "Movements" (Section 2.2.3) and Appendix A for details).

For outdoor herds, the total infectious pressure exerted by wild boar on herd i at time t was given by:

$$\Omega_i(t) = \sum_k \beta \exp\left(-\frac{d_{ik}}{\alpha}\right) I_k(t) \tag{25}$$

where $\beta > 0$ and $\alpha > 0$ are the same parameters as in the wild boar model (equation (21) and Table 51), d_{ik} is the Euclidean distance between herd i and the centre of infected wild boar patch k, and I_k is the number of infectious boar (alive and carcasses) in patch k.

2.2.2 Population dynamics

2.2.2.1 Wild boar

We assumed a constant population size among wild boar in the absence of hunting, carcass removal and ASFV-related mortality. Across Europe, wild boar breeding is typically seasonal, commencing in late autumn/early winter with peaks in November/December. Following a gestation period of 115 days, peak birthing of piglets occurs between February and April (Alves da Silva et al., 2004; Podgórski and Śmietanka, 2018; Rosell et al., 2012; Sabrina et al., 2009). Therefore, we did not account for births since the period over which projections were required (27th August 2020 until 23rd February 2021, corresponding to days 51-230) was not within the known peak birthing period for wild boar. We also did not account for natural mortality due to the short duration of the projection period relative to the average lifespan of wild boar (Herrero et al., 2008; Jezierski, 1977) and given that the predominant causes of mortality over the projection period were likely to be hunting and ASFV, both of which our model accounted for. Thus, the population of wild boar, both dead and alive, remaining in the landscape at any time could only be decreased through removal by hunting (all hunted boar were removed from the landscape) or via surveillance. For wild boar, two main types of surveillance were carried out in the island: (1) passive surveillance, which involved the removal and reporting of found wild boar carcasses, and (2) active surveillance, which involved active search for wild boar

carcasses around already detected infected carcasses. Details on the implementation of surveillance are provided in Section 2.2.5.1.4.

2.2.2.2 Pig herds

We assumed a constant population size in each herd in the absence of ASFV-related mortality, with two population dynamics processes depending on the production type of the herds: birth of susceptible pigs in farrow-to-wean and farrow-to-finish herds, and animals sent to the abattoir in finishing and farrow-to-finish herds. Natural mortality was not accounted for.

Thus, in farrow-to-wean and farrow-to-finish herds, the number of pigs leaving the herd (outgoing movements) was compensated by the entry of the same number of pigs (susceptible only). On the other hand, in finishing and farrow-to-finish herds, the number of pigs entering the herd (ingoing movements) was compensated by the same number of pigs leaving to the abattoir. Such processes were considered an acceptable approximation of the population dynamics of the pig herds given the batch system used in swine production and the timescale of the simulations.

2.2.3 Movements

2.2.3.1 Wild boar

In phase 3, to make the model more representative of wild boar movement dynamics, we implemented a threshold – the maximum infection range (MIR). This was chosen to be 8 km to reflect reports of the maximum distance travelled and the estimated home range of wild boar (Janeau et al., 1995; Podgórski et al., 2013). Consequently, an infectious wild boar in a patch A could infect other susceptible wild boar in the same patch or in another patch B if the centre of B was situated less than 8 km from the centre of A (see Figure A2, Appendix A). Similarly, a pig herd i could only be infected by infectious wild boar in a patch k whose centre was located less than 8 km from herd i (i.e., k such that $d_{ik} \leq \mathrm{MIR}$ in equation (25)). In phases 1 and 2, no threshold was set for this maximum distance (Table 52).

2.2.3.2 Pig herds

Data on pig movements up to day 50, 80 and 110 (for phases 1, 2 and 3, respectively) were provided by the challenge coordinators and therefore these pig shipments between herds were considered as deterministic (day of the shipment, source and destination herds, number of pigs shipped). Pig movements from day 51, 81 or 111 onwards (for phases 1, 2 and 3, respectively) were projected using Exponential Random Graph Models (ERGMs) to determine a pair between a source herd and a destination herd (Relun et al., 2017), and using Generalized Linear Models (GLMs) with zero-truncated negative binomial distribution to determine the number of pigs exchanged (more details are provided in Appendix A).

2.2.4 Initial conditions

2.2.4.1 Wild boar

The initial size and spatial distribution of the wild boar population in each patch was estimated using the hunting bag data and hunting rate estimates for 2019. At each phase, the model was seeded with some ASFV infections among wild boar, as observed in the synthetic data. See Appendix A for details.

2.2.4.2 Pig herds

Pig herds were distributed according to the coordinates provided. We considered all known herds in the island. The number of known pig herds changed at each phase as the number of unregistered farms identified increased (see details in section 2.1 above): 4533 for phase 1, 4537 for phase 2 and 4540 for phase 3. Each herd was initialized with susceptible pigs based on its size provided by the challenge coordinators. In all analyses, ASFV was introduced in pig herd 3594 (the first detected infected pig herd) by replacing a susceptible pig (*S*) by an exposed pre-infectious pig (*E*) at day -31, giving a median suspicion date in the model at day 0 and a median detection date at day 3, as observed in the synthetic data.

2.2.5 Disease management measures and model implementation

2.2.5.1 Wild boar

2.2.5.1.1 Fence

As part of the measures to curb the spread of the virus out of the forest area, a 300 km rectangular fence was set up around the area where ASFV had been initially detected in wild boar (ASF Challenge coordinators). The fence was operational from day 60 and was assumed to have no impact on transmission before this date. In the models we presented for phases 1 and 2, the fence was assumed to be 100% effective from day 60. However, by phase 3, the locations of some newly detected infections in the synthetic data suggested that the fence was not fully effective. Thus, we allowed for a “leaky” fence in all directions, such that ASFV could be transmitted between two patches on opposite sides of the fence if the distance between their centres was less than or equal to half the MIR (Table 52 and Appendix A). This also applied to transmission from wild boar to pig herds: in phase 3, only wild boar patches situated on the same side of the fence as outdoor herd i and satisfying $d_{ik} \leq \mathrm{MIR}$ and wild boar patches situated on the other side of the fence and satisfying $d_{ik} \leq \mathrm{MIR}/2$ were considered in the computation of the infectious pressure (equation (25)). In phases 1 and 2, only wild boar patches situated on the same side of the fence as herd i were considered.

2.2.5.1.2 Normal hunting pressure

The “normal hunting pressure” scenario involved hunting according to the usual hunting rates for a typical hunting season, which corresponds to a hunting rate of 50% of the wild boar population from day -36 to day 204 (8 months) and at a uniform rate over the period. This measure was maintained outside the fence and a 15 km-buffer zone around the fence for the entire duration of the projection period. Under this scenario, both active and passive surveillance were possible and 20% of all hunted wild boar were tested.

2.2.5.1.3 Increased hunting pressure

Within the fenced area and the buffer zone, an “increased hunting pressure” management strategy was implemented, beginning at day 60. This involved applying a hunting rate of 90% of the wild boar population (much higher than that observed in a typical hunting season) from day 60 to day 120 (2 months), at a uniform rate, to decrease wild boar density and thus slow the spread of ASFV (ASF Challenge coordinators). Under this measure, active surveillance ceased within the fence and the buffer zone, given “the potential risks posed by hunts” (ASF Challenge coordinators). However, passive surveillance was still possible. Moreover, 100% of all hunted wild boar were tested.

2.2.5.1.4 Surveillance

For model fitting, the number of boar hunted daily was estimated based on the data provided on the number of hunted boar tested daily. The proportion of hunted boar tested was 20% under normal hunting pressure and 100% under increased hunting pressure. Thus, under normal hunting pressure, the number of boar hunted daily was equal to five times the number of tested boar, whereas under increased hunting pressure, the number of boar hunted daily was equal to the number of tested boar. The number of boar carcasses found daily (by passive or active surveillance) was solely determined based on the synthetic data provided, since all found boar carcasses were tested and hence reported. According to the synthetic data provided, carcasses may persist in the island for more than one day; i.e., not all carcasses are removed via surveillance on a given day. As participating teams were blind to the synthetic data-generating process, we are unable to provide details such as the parameterization of the boar removal data provided. For details on the synthetic data-generating process, see Picault et al. (2021).

For the projection periods, no data were provided on the daily number of hunted boar and found carcasses. For these periods, we estimated the daily number of hunted boar and found carcasses based on the fractions of removed boar in the synthetic data provided; i.e., the data provided on the observed periods. Refer to Tables A9, A10, and A12 in Appendix A for detailed

descriptions on the estimation of the number of wild boar removed during the projection periods in phase 1, phase 2 and phase 3, respectively.

For both model fitting and model projections, after the number of boar to be removed had been determined, we determined the particular boar to be removed by randomly sampling from the remaining boar within a specific area of focus. Within the projection periods for phases 2 and 3, and for boar located within the fence and buffer zone, we defined the probability of removal by hunting to be dependent on a boar's infection status (this was not the case for phase 1). We assigned a higher removal probability to infected boar than to susceptible boar, such that infected boar were more likely to be hunted or found as carcasses or found as carcasses, as, we thought it reasonable to assume that infected boar were less likely to escape a hunt due to reduced activity as a result of lethargy, given the symptoms of ASF. The absolute difference in hunting probabilities for live infected boar and live susceptible boar was 0.6 in phase 2 and 0.1 in phase 3: these were chosen to ensure a high agreement between the synthetic data and simulated dynamics.

2.2.5.2 Pig herds

2.2.5.2.1 Baseline regulatory interventions

According to the challenge coordinators, disease management measures defined by European regulations were immediately implemented in Merry Island in response to the epidemic, when the first detected infected pig herd was confirmed (day 3). These regulations were originally established by the European Union (European Commission, 2002) and are now described in the new "Animal Health Law" (European Commission, 2016) and its supplement as regards rules for the prevention and management of diseases such as ASF (European Commission, 2020a).

Based on the description of the disease management measures provided by the challenge coordinators, the following measures were implemented in our model: (1) suspected pig herds were confirmed infected three days after suspicion, assuming perfect ASFV detection tests; (2) all herds with confirmed infection were culled the day after confirmation (four days after

suspicion), implemented in our model by setting all compartments to zero (including residues from dead pigs, i.e., assuming cleaning and disinfection were effective immediately); (3) after a herd was confirmed infected, a protection zone (3 km radius for 40 days) and a surveillance zone (10 km radius for 30 days) were defined, and at-risk herds that traded pigs with infected herds (ingoing or outgoing movements) within the previous three weeks were traced; (4) all movements of pigs (ingoing or outgoing) were banned for 40 days in protection zones and at-risk herds, and for 30 days in surveillance zones; (5) awareness of farmers about ASF was improved in surveillance and protection zones, as well as for at-risk herds; (6) repopulation of a culled herd was allowed 50 days after culling (except if the herd was still in a protection or surveillance zone), assuming that all pigs used for repopulation were susceptible.

In our model, suspicion of a herd was assumed to occur when two conditions were met: (1) when the mortality rate caused by ASFV during the previous 14 days in the herd was more than 6% (Andraud et al., 2019); and (2) the number of clinical or dead animals in the herd reached a minimum value of five during the previous 14 days (Halasa et al., 2016a). The minimum number of clinical or dead animals was introduced to represent more accurately the probability of detecting abnormal events, especially in small herds, where only one death could make the mortality rate exceed the threshold (Halasa et al., 2016a). Increased awareness of farmers in protection and surveillance zones and in at-risk herds was represented in our model by reducing the minimum number of clinical or dead animals required for detection to one (Halasa et al., 2016a).

2.2.5.2.2 Additional interventions (phases 2 and 3)

During phase 2, additional disease management strategies in pig herds were incorporated into the model as asked by the challenge coordinators (see Appendix A for more details): (1) preventive culling of all herds in a protection zone (“cullPZ”); (2) increasing the size of the surveillance zone from 10 km (the standard radius used) to 15 km (“incrSZ”); (3) preventive culling of all pig herds located at less than 3 km from positive wild boar carcasses (“cullWB”); and (4) preventive culling of all at-risk herds (“cullTR”). Those additional interventions were

implemented in forward projections during phase 2, i.e., from day 81 to day 110. During phase 2, pig herds preventively culled before detection in scenarios cullPZ, cullWB and cullTR were not tested (Table 52). Culling was assumed to take place 24 hours after the event triggering the intervention, as for confirmed herds in baseline interventions.

During phase 3, cullWB was implemented starting day 90 according to the challenge coordinators. Preventive culling happened 5-7 days after a wild boar case was confirmed, and tests were performed rapidly in all culled herds, providing results the day after (Table 52).

2.3 Analyses

2.3.1 Comparison of scenarios

Using model simulations, we compared epidemic outcomes (number and locations of cases) under the range of scenarios discussed, to determine the effectiveness of each at limiting the epidemic.

2.3.2 Probability of epidemic fade out by day 230

A key question of interest posed by the challenge coordinators in phase 3 was how likely the epidemic was to fade out by day 230 given the following conditions: (1) a cessation in increased hunting pressure at day 120 (due to a reduction in reported incidence), (2) end of the hunting at day 204 (usual last day of hunting on the island), and (3) possibility of passive discovery of wild boar carcasses beyond day 204. To estimate the probability of fade-out, we simulated from our model under these conditions and computed the proportion of simulations having at least one case by day 230. This was done for both wild boar and pig herd populations.

2.3.3 Parameter estimation

The wild boar model was calibrated using Approximate Bayesian Computation (ABC) (Beaumont et al., 2002). In phase 1, the type of ABC algorithm employed was ABC-Sequential Monte Carlo with M-nearest neighbours (Minter and Retkute, 2019; Toni et al., 2009) while in phases 2 and 3, the ABC rejection algorithm (see Toni et al. (2009)) was employed.

In all phases, the transmission parameter β was estimated. In phases 2 and 3, to improve the runtime of the estimation algorithm, the scale parameter α of the dispersal kernel was fixed based on its estimated value at Phase 1 and results from some trial runs of the model.

The wild boar summary statistics used in the ABC estimation were: (1) the daily number of detected infected wild boar, and (2) the area of the minimum convex polygon enclosing the locations of infected patches. By choosing these summary statistics, we sought to make our model fit reflect well both the size and spatial extent of the epidemic in wild boar, as in the synthetic data. The parameter values producing simulated summary statistics closest to the summary statistics as computed from the synthetic data provided were retained for model predictions. The tolerances used in the ABC were chosen based on an iterative sequence of trial runs which compared simulated model outputs to the synthetic data.

Parameters exclusively associated with the pig herd model were derived from published estimates (Table 51). After a graphical comparison between the synthetic data provided and the simulated daily and cumulative numbers of detected infected pig herds over time at each phase, the same transmission parameter values for transmission from wild boar to pigs in outdoor herds were used as those calibrated for wild boar-to-wild boar transmission (α and β).

2.3.4 Simulations and outputs

During the challenge, the number of stochastic repetitions decreased from 500 for phase 1, to 72 for phase 2 and 32 for phase 3 because of constraints imposed by real-time analysis. However, the results presented in this paper were expanded to include 500 stochastic repetitions for each phase.

For the wild boar model, the simulated period was from day 1 in phases 1 and 2, but from day 60 in phase 3, due to computational constraints. For the pig herd model, the simulated period was from day –59 (when data on pig movements started) in all phases. Each repetition corresponded to a given set of parameter values retained by ABC (α and β in phase 1, only β in phases 2 and 3). In addition, model stochasticity was driven by drawing events randomly from probability distributions.

For wild boar, model outputs across all phases were the daily number of detected/infected wild boar and the locations of infected wild boar patches. In phases 2 and 3, additional outputs were infected wild boar locations. For pig herds, model outputs were the daily number of suspected/confirmed/infected herds, and the probability of suspicion/detection/infection for each herd (expressed as the proportion of simulations where a given herd was suspected/detected/infected). Model outputs were expressed as the median of the simulations and the associated 95% equal-tailed credible interval (CrI), using the 2.5% and the 97.5% percentiles of the simulations as lower and upper bounds of the 95% CrI, respectively. Additional details on model outputs are provided in Table A8, Appendix A.

2.3.5 Sensitivity analyses

To assess the sensitivity of our model to changes in parameter values and assumptions, we conducted two sensitivity analyses.

First, we assessed the influence of the MIR, the scale parameter of the dispersal kernel α, the duration of infectiousness in wild boar carcasses, and the duration of infectiousness in live boar on the daily number of infections and detected cases in wild boar and pig herds. For this analysis, we focused on phase 3, from day 60 to 110, corresponding to the period over which the phase 3 model was fitted. We chose to use the phase 3 model since it is the only model which incorporates the MIR. We considered values ranging from 2 km to 20 km for the MIR; from 0.6 km to 1.2 km for α; from 10 days to 130 days for the duration of infectiousness of wild boar carcasses (Fischer et al., 2020; Mazur-Panasiuk and Woźniakowski, 2020); and from 5 days to 14 days for the infectious period in live boar (Gervasi et al., 2020; Gervasi and Guberti, 2021; Halasa et al., 2019; Hayes et al., 2021; O'Neill et al., 2020; Pepin et al., 2020).

Second, we assessed the sensitivity of projections for the number of detected infections in wild boar and pig herds by day 140 to the level of efficacy of three interventions: (1) fencing; (2) testing of hunted or found wild boar post-removal; and (3) culling of pig herds located less than 3 km away from positive wild boar. For each of these interventions, we assessed the changes in the number of detected infected animals if the parameters associated with these

interventions were reduced to 75% and 50% of their baseline values. This analysis was performed using a full factorial design (Saltelli et al., 2008) in which there were three factors (the interventions parameters) and three levels for each factor (100%, 75%, and 50%). Thus, 27 (=3^3) combinations of intervention efficacies were assessed. For testing of wild boar and culling of pig herds, the parameters controlling efficacy were the proportion of tested wild boar and the proportion of culled pig herds, respectively. For fencing, the parameter controlling efficacy was the permeability of the fence. During phase 3, ASFV could be transmitted between patches i and j on opposite sides of the fence if $d_{ij} \leq \mathrm{MIR}/2 = 4$ km. Here, we decreased the efficacy of the fence by increasing its permeability, using $d_{ij} \leq \mathrm{MIR}/(2 \times 0.75) = 5.3$ km and $d_{ij} \leq \mathrm{MIR}/(2 \times 0.5) = 8$ km instead.

For each parameter X assessed, we compared model outcomes under different values of X, including the baseline value employed in our model. For each value of X studied, the sensitivity analyses involved running 100 stochastic repetitions of the model. In these model simulations, all other parameters and all model assumptions, including control measures, were as in the baseline model. We then computed the median and 95% CrIs for each outcome across the 100 stochastic repetitions.

3 Results

3.1 Parameter estimation and model fit

Parameter estimates at each phase are provided in Table 51. Our model fitted well to the temporal and spatial dynamics of the epidemic (Figure 51 and Table 53; Figure B1, Appendix B). To evaluate the ability of our model projections to capture the dynamics of the epidemic, we also compared model projections for the detected number of cases in wild boar and pig herds during phase 1 (up to day 78) and phase 2 (up to day 110) to the synthetic data provided by the challenge coordinators after these two phases were completed. We were not provided with synthetic data corresponding to the projection period for phase 3 (beyond day 110), thus precluding comparison of our projections in that phase with synthetic data. The

95% CrIs for the number of detected infected pig herds and wild boar captured the synthetic observations in phase 1 (Table 54). In phase 2, the 95% CrIs for the number of detected infected pig herds captured the number observed in the synthetic data, although the corresponding statistic for the number of detected infected wild boar did not; the median estimate for wild boar overestimated the number observed in the synthetic data by 7.7% (Table 54).

Although ASFV was seeded in both wild boar and pig herds, pig herd incidence was driven by the wild boar epidemic, as illustrated in Figure B2, Appendix B. Indeed, in the absence of ASFV transmission from wild boar to pig herds, the cumulative number of detected infected pig herds up to day 230 remained very low (median: 2, 95% CrI: (2-7)).

3.2 ASF management strategies

3.2.1 Fencing and increased hunting pressure

The challenge coordinators were interested in the difference in effectiveness between the scenario involving the implementation of the fence alone and that involving the implementation of the fence combined with increased hunting pressure within the fence (and from phase 2 also in the buffer zone; see Table 52). For all phases, we report model projections of the daily number of detected infected wild boar and the daily number of detected infected pig herds under the increased hunting pressure and normal hunting pressure scenarios (Figure 52). In general, our model projections showed a better efficacy of the combination of fence with increased hunting pressure in comparison with fence and normal hunting pressure (Figure 52, Table 53).

In wild boar, for phase 1, there were 90% more detected cases under increased hunting pressure compared to normal hunting pressure (Table 53). However, for phases 2 and 3, there were more cases under normal hunting pressure than under increased hunting pressure: the projected median estimates for normal hunting pressure were 1.8% and 131% higher than corresponding estimates for increased hunting pressure, for phases 2 and 3, respectively (Table 53). The projected number of detected infected pig herds was very similar for both

scenarios in phase 1 (Figure 52, Table 53). In phase 2, the projected median number of detected infected pig herds was 7% lower for increased hunting pressure than for normal hunting pressure (Figure 52, Table 53). It was only in phase 3 that increasing hunting pressure had a strong impact, with a 56% lower median estimate of detected infected pig herds compared to the normal hunting pressure scenario (Figure 52, Table 53).

3.2.2 Additional interventions in pig herds

The model projections showed that culling all pig herds in protection zones ("cullPZ"), culling all herds that have traded pigs with an infected farm less than three weeks before detection ("cullTR"), or increasing the size of the surveillance zone from 10 km to 15 km ("incrSZ") all had a negligible impact on the number of infected herds and detected infected herds compared to the baseline management strategies in pig herds (Figure 53; Figure B3, Appendix B). However, culling of all pig herds located less than 3 km from positive wild boar carcasses ("cullWB") led to 4 fewer infected herds on average, compared to the baseline management strategies, a 18.5% reduction over a 30-day period (Figure 53). This reduced number of infected herds was obtained by culling 65 more herds on average compared to the baseline management strategies, a 422% increase over a 30-day period.

3.3 Probability of epidemic fade-out by day 230

Our model simulations showed the persistence of the virus within the population by day 230 in all projections (Figure 54), given the new disease management measures introduced at day 120. The estimated daily numbers of detected cases beyond day 120 were generally lower than had been observed in the synthetic data at the start of the increased hunting pressure activities (day 60) and followed a steady trend up to day 204, after which even fewer cases were detected daily, given the end of the hunting season. The probability of fade-out in pig herds depended on the probability of fade-out in wild boar (Figure B2, Appendix B). Indeed, as long as the virus persists within the wild boar population, further infections of pig herds are to be expected.

3.4 Sensitivity analyses

3.4.1 Sensitivity analysis to spatial parameters and durations of infectious periods

There was no substantial difference between the trajectories for the daily number of detected infected boar corresponding to MIR values of 8 km, 14 km and 20 km, although there was a marked difference between these trajectories and that corresponding to a MIR of 2 km (Figure 55A). Increasing the MIR from 2 km to 8 km resulted in a 187% (95% CrI: 160%-206%) increase in the number of detected infected boar within the period considered (days 60-110), whereas increasing from 8 km to 14 km resulted in only a 2.02% (95% CrI: -5.4%-12%) increase (Table 55). Similarly, the number of detected infected pig herds increased by 100% (95% CrI: 61%-152%) when increasing the MIR from 2 km to 8 km but did not change further for values above 8 km. Similar results as for detected infected boar and pig herds were obtained when considering the number of infections (detected or not: Figure C1A, Appendix C).

For the duration of infectiousness in boar carcasses, we observed a similar trend where the results changed only for the smallest parameter value. Indeed, there was no notable difference between the median trajectories corresponding to the 50-day, 90-day and 130-day durations, but the trajectory corresponding to a 10-day duration was slightly lower starting from day 70 (Figure 55C). However, CrIs corresponding to estimates for all parameter values were largely overlapping (Figure 55C, Table 55). Similar results were observed for the number of infections and the number of detected infected pig herds (Table 55 and Figure C1C, Appendix C).

The trend was however different for the scale parameter of the dispersal kernel, α (Figure 55B), and the duration of infectiousness in live boar (Figure 55D). For these parameters, larger parameter values resulted in larger values of the daily number of detected infected wild boar. This was especially true for the scale parameter α, for which the number of detected infected wild boar increased by 190% (95% CrI: 169%-212%) from 0.6 km to 1.2 km, and the number of detected infected pig herds increased by 140% (95% CrI: 82%-204%) from

0.6 km to 1.2 km (Table 55). A similar trend was observed for the number of infected wild boar (Figure C1B, Appendix C).

Decreasing the infectious period of live boar in the baseline model (14 days) by 4 days, 7 days, and 9 days resulted in a decrease of 16% (95% CrI: 10%-23%), 30% (95% CrI: 24%-37%) and 40% (95% CrI: 35%-45%), respectively, in the number of infected detected boar, compared to baseline (Figure 55D, Table 55). However, decreasing the infectious period in live boar led to no substantial changes in the number of infected wild boar (Figure C1D, Appendix C) nor in the number of detected infected pig herds (Table 55). See Section 4.2 of the “Discussion” for an interpretation of these results.

3.4.2 Sensitivity analysis to efficacy of management interventions

Results on the sensitivity of the number of detected infections to the level of intervention efficacy are presented in Table 6. For any fixed fence efficacy level, decreasing the testing fraction led to fewer detected infections in wild boar. On the other hand, for a fixed testing fraction for wild boar, the number of detected boar and pig herds did not vary substantially with varying fence efficacy – credible intervals for estimates were largely overlapping. Given any fixed combination of intervention efficacy levels in wild boar (e.g., fence efficacy as 100% and testing efficacy as 75%), varying the fraction of pig herds culled if found less than 3 km away from positive wild boar (cullWB) led to only negligible changes in the median estimates of the number of detected pig herds. Across levels of cullWB, the credible intervals of estimates were largely overlapping for all combinations of fence and testing efficacies considered.

4 Discussion

We have developed a stochastic spatiotemporal model describing the transmission dynamics of ASF in a multispecies context involving wild boar and domestic pigs. Our model captured the shape of the epidemic trajectory, as reflected in the synthetic data, as well as its spatial characteristics (Figure 51; Table 53; Table 54; Figure B1, Appendix B). Furthermore, the

model was complex enough to allow for the incorporation of a range of disease management measures and for the estimation of their respective effects on the epidemic trend (Figure 52 and Figure 53, Table 53).

4.1 What do our results show and what do they mean?

4.1.1 Key point 1: Increased hunting pressure effective, long-term evaluation more beneficial

To inform recommendations for ASF management measures in the wild boar population – assumed to be the reservoir for ASFV in the island we considered – we evaluated the effectiveness of an increased hunting pressure scenario and a normal hunting pressure scenario, both including a fenced area to restrict wild boar movement beyond an identified epicentre. Our model results showed a superior efficacy associated with the increased hunting pressure scenario (Figure 52, Table 53). It is worthy of note that the benefits (reduction in the number of infected boar removed) realized under the increased hunting pressure scenario were more apparent in the longer term, in both the wild boar and pig herd populations (Figure 52). For wild boar, the benefit of increased hunting pressure could only be seen in phases 2 and 3 (Figure 52B-C), where the number of detected infected boar decreased despite testing more (as 100% of hunted boar within the fence and buffer zones were tested in the increased hunting pressure scenario, compared to only 20% in the normal hunting pressure scenario). For pig herds, increased benefit in the longer term can be visually observed in the cumulative curves in Figure 52G-I, where the divergence between the scenario curves is seen to increase as the epidemic progresses. In the face of emerging threats such as ASF, where there is typically a haste to suppress disease spread, mechanisms which do not prove highly effective in the short term might be quickly abandoned or less favoured. These results suggest that the timescale over which different interventions are evaluated may influence the evaluation outcomes. In particular, the difference in efficacy between two interventions may be negligible when the interventions are evaluated over a short time window, but this difference may become considerably larger when the interventions are

evaluated over a longer window. Consequently, we recommend that rather than comparing interventions over a fixed time window (e.g., 30 days, as in phase 1), which may not be enough to see an effect, interventions are compared based on the time it takes these interventions to reach a certain level of efficacy as defined by example, the public health manager.

4.1.2 Key point 2: Preventive culling around positive wild boar was effective in pig herds

As done for wild boar, we compared various ASF management measures in pig herds, that could complement the baseline interventions defined by the EU and that were implemented in Merry Island. These additional measures included increasing the size of the surveillance zone from 10 km (the standard radius used) to 15 km, or the preventive culling of herds either in a protection zone, defined as being at-risk (based on previous trade with infected herds), or located at less than 3 km from positive wild boar (Table A11, Appendix A). These measures were evaluated and compared during phase 2 of the challenge.

Increasing the size of the surveillance zone by 5 km was not effective in reducing the number of infected or detected pig herds (Figure 53; Figure B3, Appendix B). We also found that preventive culling of herds connected to detected infected herds had a negligible impact on the number of infected and detected pig herds (Figure 53; Figure B3, Appendix B). Similar to our results, increasing the size of the surveillance zone or pre-emptive culling around infected herds were not predicted to improve the management of a hypothetical ASFV epidemic in Denmark (Halasa et al., 2018, 2016c). In our case, these results can be explained by the fact that incidence in pig herds was largely driven by transmission from wild boar (Figure B2, Appendix B). Therefore, these scenarios strictly relating to pig-to-pig transmission had only limited impact.

In contrast, culling pig herds located less than 3 km away from positive wild boar decreased the number of infected pig herds by 18.5% in one month (Figure 53). This type of preventive culling was more effective as it prevented boar-to-pig transmission, by depleting pig herds before they were exposed to transmission from wild boar. However, this scenario required the

culling of 65 additional herds in a month compared to the baseline scenario. Although the costs of disease management interventions were not directly evaluated in our model, the costs associated with this scenario would probably be substantial. The cost-benefit ratio of this strategy should therefore be evaluated by comparing the costs of culling additional herds with the benefits of preventing ASF in a few herds.

One possible refinement of this scenario would be to preventively cull the herds most at-risk of transmission from wild boar, i.e., outdoor herds. Here, all herds (indoor and outdoor) were indiscriminately culled, whereas only outdoor herds were assumed to be exposed to transmission from wild boar. By culling only outdoor herds close to positive wild boar, this scenario would be expected to produce similar benefits while decreasing the number of preventively culled herds, hence reducing the costs and potentially reducing delays required to implement such culling. Double fencing of outdoor pig herds as an alternative to keeping FRPs has been implemented as part of the recent eradication programme in Sardinia (Viltrop et al., 2021). Whilst the epidemiology of ASFV in Sardinia is different to that of Merry Island as FRPs rather than wild boar are considered the main drivers of transmission, double fencing of outdoor pig farms could also be considered as an alternative or addition to culling as a means of reducing transmission between wild boar and outdoor pig herds. Scenarios such as these could have been evaluated using our model; however, given the time restrictions imposed in the challenge to mimic real-time analysis and decision making, we restricted our analyses to the scenarios asked by the challenge coordinators.

4.1.3 Key point 3: ASFV persistence beyond day 230 and what this means for disease control

Concerning the probability of epidemic fade-out, our model estimates suggest the strong likelihood of the persistence of ASFV in the landscape by day 230 (Figure 54), translating to a probability of incidence among pig herds, since the epidemic in pig herds is sustained by that in wild boar (Figure B2, Appendix B). The fact that our simulations stopped at the beginning of the peak birthing season (February – April (Alves da Silva et al., 2004; Podgórski

and Śmietanka, 2018; Rosell et al., 2012; Sabrina et al., 2009)), also suggests a potential for endemicity of the virus in the landscape with seasonal epidemics, since the peak of introduction of new susceptible individuals into the population represents increased opportunities for transmission (Altizer et al., 2006). In addition, boar piglets have been seen to survive for longer periods after infection compared to adult boars (Sánchez-Cordón et al., 2019), meaning an increased potential for effective contacts per infected individual and hence a higher chance of epidemic take-off.

However, the simulated epidemic which was used to provide the data used in the challenge showed a decline in real incidence in wild boar from around day 35, down to almost no new cases by day 230 (ASF Challenge coordinators). This discrepancy between our results and the original model could have originated from the differences in assumptions. For instance, ASFV was introduced into a single wild boar in the original model 112 days before the first detected case (ASF Challenge coordinators). In our model, ASFV infections were seeded in wild boar at day 1 for phases 1 and 2 or at day 60 for phase 3, based on the number of infected boar in the synthetic data provided (Appendix A). As the number of seeded infections was assumed based on the number of infected boar as observed in the synthetic data and not estimated, this number could have been underestimated. This could have resulted in a temporal shift of the epidemic according to our model, whereby day 230 would be in earlier stages of the epidemic than observed in the “real” trajectory, thus overestimating virus persistence. Estimating the number of infections at the beginning of the simulations or the date of introduction of the virus could represent possible refinements to avoid this issue. Another possible explanation could be the spatial spread of the virus. Spatial diffusion is dependent on the probability of the virus reaching new areas with susceptible individuals. Differences in parameter estimates or in spatial structure (patches in our model versus individual boar in the original model) could explain a faster diffusion in our model compared to the original one, increasing the chances of reaching new areas with susceptible boar and therefore increasing virus persistence.

However, virus persistence, as predicted by our model, is more reflective of the current situation and challenges being faced by many countries within Europe. Wild boar play an important role in the epidemiology of ASFV in Europe with current evidence suggesting that ASFV is maintained at low prevalence in the wild boar population with the persistence of ASFV within wild boar carcasses and the associated environmental contamination contributing to the maintenance and spread of disease (Chenais et al., 2019). In areas where ASFV is present in local wild boar populations, transmission to pig herds may occur via direct contact between wild boar and outdoor pig herds or may occur via human-mediated introduction from the contaminated local environment (Chenais et al., 2019). Since its re-introduction to Europe in 2007, only two countries – the Czech Republic and Belgium – have managed to eradicate ASFV when it has been present in wild boar (European Food Safety Authority et al., 2021; Miteva et al., 2020; Sauter-Louis et al., 2021a). In both countries, ASFV was restricted solely to wild boar following a focal human-mediated introduction. In the Czech Republic the closest infected wild boar to the first confirmed wild boar case was over 300km away, whilst in Belgium the distance was over 800km (Sauter-Louis et al., 2021b). This focal introduction is considered an important factor in the success of interventions within both the Czech Republic and Belgium (Sauter-Louis et al., 2021b). In contrast, ASFV is endemic within the resident wild boar population in some eastern European countries, which hampers control efforts (Chenais et al., 2019). The control measures utilised in the Czech Republic and Belgium reflect measures currently recommended by the EU when a focal introduction within wild boar has occurred in a previously disease-free area (European Commission, 2020b; Miteva et al., 2020). Three separate zones are demarcated – a core zone, a buffer zone and an intensive hunting zone (European Food Safety Authority et al., 2018; Miteva et al., 2020). The core zone is the area within which ASFV-positive boar have been identified. This area is fenced to control the movement of the wild boar with the goal of reducing disturbance and avoiding dispersal of infected animals over a wider area. Mortality associated with ASFV is allowed to occur and carcasses promptly removed. During the period of active ASFV transmission, it is recommended that boar are undisturbed within both the core and buffer zones. Once the

epidemic starts to decline, active population management is recommended under strict biosecurity. Within the intensive hunting zone (which is the outermost of the three zones), the goal is to reduce the population of wild boar to below a level at which transmission of ASFV cannot be sustained. In Belgium, in addition to measures targeted at wild boar, domestic pigs within the infected area were also culled at the start of the outbreak (Global Framework for the Progressive Control of Transboundary Animal Diseases, 2020; Mauroy et al., 2021). Following the success of these strategies in Europe, a similar approach has been adopted in South Korea but has met with variable success. Differences between counties in the speed and method of implementation of control measures such as fencing and culling of wild boar are considered likely to have contributed to this variation in success (Jo and Gortázar, 2021). Breaches in biosecurity are also suggested to have contributed to both local spread and long-distance translocations of the disease (Jo and Gortázar, 2021). The challenge presented by ASF management highlights the importance of developing accurate mathematical models of ASFV transmission in wild boar and domestic pigs, to improve our understanding of ASFV transmission dynamics and to evaluate potential disease management strategies in various situations and locations.

4.2 What factors influenced model dynamics?

The sensitivity analysis allowed to gain insights on the impact of a few selected key parameters and assumptions on the infection and detection dynamics, namely (1) the limit in wild boar movements introduced during phase 3 (MIR), (2) the value of the scale parameter (α) of the transmission kernel, which was fixed in phases 2 and 3, and (3) the duration of infectiousness in live and dead boar.

We found that the detected incidence was largely unaffected by changing MIR values when MIR $\geq$ 8 km (Figure 55A). To understand this, it is helpful to consider the value of the dispersal kernel (where $\alpha = 1$ km as in the baseline model): both the value of the dispersal kernel and, consequently, the infectious pressure exerted on a susceptible patch j by an infectious patch i, decreases with increasing distance between patches (equation (21)). Thus, although the

MIR increases, resulting in an increase in the number of possible patches j that could be infected by i, the infectious pressure exerted by i on patches located at least 8 km away is negligible (value of dispersal kernel for $d_{ij} =$ 8 km is 3.3×10^{-4}), hence such long-distance infection events are unlikely in the model. Consequently, increasing the MIR beyond 8 km does not contribute substantially to the number of new infections, as observed in Figure 55A. Hence, fixing the MIR at 8 km did not artificially restrict the dynamics.

Larger values of α led to larger estimates for the detected incidence (Figure 55B and Table 55). Indeed, given constant β, d_{ij}, and the prevalence in patches i and j, larger values of α will result in higher infectious pressures on a susceptible patch j (equation (21)) and hence more infections (Figure C1B, Appendix C), and consequently, detections, than would be realized with a smaller value of α.

When the duration of infectiousness in carcasses was 50 days or more, there was almost no sensitivity of either infection or detection dynamics to changes in the values of this parameter (Figure 55C; Figure C1C, Appendix C). This is due to the fact that once boar became carcasses, they persisted in the landscape no more than 43 days on average (by day 110), a consequence of model assumptions and the removal dynamics as explained in Section 2.2.5.1.4. That is, an average boar carcass gets removed from the landscape before the end of its 90-day infectious period. Thus, values larger than 43 days will be expected to produce similar dynamics. However, values smaller than 43 days will be expected to produce different dynamics; in particular, the number of daily infections and consequently, detections will be generally lower, as infectious carcasses spend less time in the landscape.

Finally, we found that when the length of the infectious period in live boar was assumed to be shorter than 14 days (as in the baseline model), the detected incidence was generally lower than realized with the baseline model (Figure 55D). Indeed, the more days infectious boar spend alive, the higher the proportion of infected boar among all hunted boar, given that within the period considered (day 60-day 110), the major mode of detection of infected boar was hunting. The graph of the corresponding dynamics for all infections (i.e., including undetected

infected boar; Figure C1C, Appendix C) reveals that compared to the detection dynamics, infection dynamics were less sensitive to changing values of this parameter. The number of days an infected boar spends alive (14 days in the baseline model) is expected to influence detection dynamics more than it does the infection dynamics because: (1) the bulk of detections targeted live boar; hence, increasing the lifespan of infected boar means a higher probability of detecting an infected boar; and (2) shortening the duration of infectiousness as a live boar only has a small impact on the overall duration of infectiousness (because the duration of infectiousness in carcasses is much higher: 90 days in the baseline model), and hence on the overall contribution of wild boar (alive and dead) to transmission.

The sensitivity analysis also allowed us to assess the influence of efficacy of interventions on model projections. Interventions assessed were the fence, wild boar testing and culling of pig herds located less than 3 km away from positive wild boar. The analyses showed that decreased testing resulted in fewer infected detected boar (Table 6), as expected, and increased permeability of the fence did not appear to result in an increase in the number of detected infections in boar (Table 6).

4.3 What challenges did we face?

The main challenge faced in model implementation concerned computation time. The complexity of the models, coupled with the increasing amounts of data as the modelling challenge progressed, made simulations and parameter estimation slow. This efficiency drawback was even more evident during the early stages of phases 2 and 3 for two reasons: (1) in these phases, we included information on individual boars and locations because this level of granularity was needed for the implementation of pig management strategies, such as the culling of pig herds less than 3 km away from an infected wild boar, and (2) candidate models had to be iteratively tested prior to parameter estimation. To mitigate this issue, we employed three approaches. First, algorithms were parallelized where possible and useful, taking advantage of high-performance computing clusters. Second, cross-language programming was utilised where needed. Although the main programming language was R,

some sections of the model were written in the faster C++ language to improve the overall speed. Third, the final model (at phase 3) was fitted to data from day 60, rather than from day 1. (This choice likely contributed to the accuracy of the phase 3 projections: in a previous epidemic modelling challenge, it was observed that models fitted to more recent data performed better than those fitted to data over the entire observed period (Viboud et al., 2018)). Still, the computational resources required were substantial (see Table A7, Appendix A for algorithm runtimes). It is crucial, particularly in real-time analysis of epidemics, for modellers to have efficient tools in order to provide timely evidence-based recommendations for disease management. Therefore, more work is required on the efficient design of epidemic models to minimize computational burden upon implementation. Also, work to develop highly efficient parameter estimation methods which have the potential to scale with large datasets and complex models will be useful for real-time epidemic response.

4.4 How could the modelling approach/choices be improved?

Since we constructed the model rapidly during a hypothetical animal health emergency, the modelling approach presented here can be improved in a number of ways. First, the component of the model describing transmission dynamics in wild boar could be made more realistic by including a latent compartment, as in the pig herd model. The sensitivity analysis on the duration of infectiousness in live boar may be considered an approximate test on the length of a latent period on infection dynamics: one may think of the baseline model as allowing for no latent period and of the alternative models as allowing for a latent period of D days, where D is the decrease in infectious period between the baseline and the alternative model. The difference in the number of infected detected boar between the baseline model and the alternative models (decrease in infectious period by 4, 7 and 9 days) was notable – the lower the infectious period, the lower the number of infected detected boar relative to the baseline (Figure 55, Table 55). The absence of a latent period in the wild boar model may therefore explain the overestimation in the number of infected detected cases in phase 2 (Table 54 and Table 55).

Second, our model could be fitted to pig herd incidence, to better characterize infection dynamics between herds. We were not able to fit our model to pig herd data because the data were restricted to the number of detected infected pig herds, which was very low especially during the early phases of the challenge. Incorporating the analysis of data on pig herds could have allowed the separate estimation of α and β parameters for boar-to-boar and boar-to-pig transmission. However, the close similarity between model projections and data for pig herds (Table 53; Figure B1, Appendix B; Table 54) show that the use of common parameters for boar-to-boar and boar-to-pig transmission was sufficient for the purposes of our model. In addition, this avoided the need to perform ABC for both components of the model, which would have increased an already long computation time. Parameters for within- and between-herd transmission were based on experimental infections (Gallardo et al., 2017; Guinat et al., 2016b), previous modelling work (Halasa et al., 2016c, 2016a) or adapted from knowledge from classical swine fever virus. More detailed data, for instance on the number of infected or dead pigs in each herd, could have been useful to estimate within-herd parameters (Guinat et al., 2018). This kind of data could be collected when facing a real ASF epidemic to better inform mathematical models used.

4.5 How can the projections be improved?

Our projections could be improved by utilising multi-model ensembles as these have consistently demonstrated superior prediction abilities and lower variance, on average, compared to single models for epidemic forecasts (Johansson et al., 2019; McGowan et al., 2019; Reich et al., 2019; Viboud et al., 2018), deriving advantage from their ability to incorporate various signals from their constituent models, each of which may capture a distinct combination of system characteristics (McGowan et al., 2019). In the context of modelling challenges or real-time analysis of epidemics, the limited time available for analysis may make it challenging to develop multiple, diverse models needed for a good ensemble. For some modelling challenges, an ensemble based on the presented models have been developed (for

example, (McGowan et al., 2019; Viboud et al., 2018)) and such ensembles could serve as useful tools for informing disease management in the event of a real epidemic.

4.6 Comparison to previously published modelling studies

The pig herd model used within this study was broadly based on the models reported by Halasa et al. (2016c, 2016a). For within-herd transmission, the main modification that was implemented within our model related to the duration of the latent and infectious periods. We based these on experimental data reported by Guinat et al. (2016b) rather than on expert knowledge and we incorporated uncertainty in these parameter values as in Vergne et al. (2021). As in previous studies (Guinat et al., 2018; Halasa et al., 2016a), we assumed homogeneous mixing within herd, i.e., ignoring the impact of herd structure on ASF transmission. Although this may not represent adequately the reality for some highly-structured pig herds, this assumption was mainly the result of an absence of within-herd epidemiological data and a lack of information on how pig herds were structured. The impact of this assumption on within- and between-herd transmission remains to be assessed, but would require detailed epidemiological data to allow the estimation of multiple within-herd transmission parameters (Guinat et al., 2018, 2016b).

For between-herd transmission, a number of modifications were implemented. We only considered disease spread via animal movements and via local transmission, as these were the main drivers of between-herd transmission in Halasa et al. (2016c) and Andraud et al. (2019). We therefore assumed transmission by indirect contacts (e.g. via people visiting the farm, trucks moving animals to abattoirs, or feed trucks) to be negligible, except for local spread within a 2-km radius (e.g. via shared material). For spread via animal movements, instead of computing probabilities of virus transmission via movements (Halasa et al., 2016c), we explicitly modelled animal movements as a potential source of introduction (e.g., as in Brooks-Pollock et al. (2014)), using the synthetic movement data provided and projected movements using ERGMs. For local transmission, we used a continuous function of distance

to represent the decreasing probability of transmission with increasing distance, instead of using discrete values for certain distance ranges as in Halasa et al. (2016c).

The wild boar model was developed independently and was not based on any previously published modelling studies. As noted in Hayes et al. (2021), until 2020 the majority of the published ASFV transmission models for wild boar were based on Lange and Thulke's ASF model (Halasa et al., 2019; Lange, 2015; Lange et al., 2018; Lange and Thulke, 2017, 2015; Thulke and Lange, 2017) or parameterized as per that model (Croft et al., 2020). Our model is similar to that by Lange and Thulke (2017) in that it is a spatially explicit model. However, whilst many of the published wild boar ASF modelling studies include detailed demographic information (age and sex of individual boar, births, sub-adult dispersal, annual reproduction, litter sizes and mortality) (Croft et al., 2020; Gervasi and Guberti, 2021; Halasa et al., 2019; Lange, 2015; Lange et al., 2018; Lange and Thulke, 2017, 2015; O'Neill et al., 2020; Pepin et al., 2020; Thulke and Lange, 2017) we chose to simplify the demographic processes included within our model due to the short time-frame modelled within the ASF Challenge.

The average duration of infectiousness for live infected wild boar used in published models is typically 5-7 days (Croft et al., 2020; Gervasi et al., 2020; Gervasi and Guberti, 2021; Halasa et al., 2019; Lange, 2015; Lange and Thulke, 2017, 2015; O'Neill et al., 2020; Pepin et al., 2020; Thulke and Lange, 2017), a considerably shorter period than that used within our model (14 days) and this may have contributed to our overestimation of the number of cases in wild boar.

The duration of infectiousness of carcasses is variable across studies and varies from 4 weeks (Lange and Thulke, 2017) to 12 weeks (Gervasi and Guberti, 2021). The 90-day period used in our model would thus be at the upper end of this range. More recently, studies have varied the rate of carcass decomposition by season to reflect different seasonal rates of carcass decomposition (Gervasi and Guberti, 2021; Pepin et al., 2020; Thulke and Lange, 2017). Another study has demonstrated the influence of temperature and environmental conditions on ASFV persistence in carcasses (Fischer et al., 2020; Mazur-Panasiuk and Woźniakowski, 2020). The projection periods for the ASF modelling Challenge ran from August to February

and thus these seasonal and temperature variations in the duration of infectiousness of carcasses could have been considered in our model.

Prior to 2020 (when the ASF Challenge started), there had been a lack of diversity among ASFV models in both domestic pigs and wild boar although the situation has been improving (Hayes et al., 2021). Our model, alongside the other models produced in the ASF Challenge, provides a valuable contribution to increasing the diversity in the ASFV modelling literature. The number of studies modelling transmission between wild and domestic hosts remains small (Pietschmann et al., 2015; Pollock et al., 2021; Taylor et al., 2021; Yoo et al., 2021). Given the importance of wild boar in the transmission of ASFV in Europe, the multi-host nature of our model is one of the major strengths of our study.

5 Conclusions

In summary, we have developed a framework for modelling ASFV transmission during outbreaks. The model can be parameterized in real-time during outbreaks and refined as additional outbreak data become available. The model can be used to generate forward projections and to predict the effectiveness of different proposed disease management strategies.

For the simulated epidemic on Merry Island, our model indicated that transmission between wild boar (and from wild boar to pig herds) was the main driver of epidemic dynamics. Effective control measures included the construction of a fence around the main area of the island with high prevalence, following by increased hunting of wild boar both within and near the fenced region. Culling of pig herds was generally not an effective control strategy, except in regions with substantial numbers of infections in wild boar. This is because there was only a low risk of transmission through the pig trade network. Our model predicted that the virus is likely to persist in future on Merry Island, at least in the short to medium term.

An important general finding is that it is important to consider the timescale over which different control strategies are evaluated: in particular, the difference in efficacy between two interventions may be negligible when the interventions are evaluated over a short time window

but this difference may become considerably larger when evaluated over a longer time window.

Further refinement of our modelling framework is necessary going forwards. Nonetheless, we have demonstrated the potential for this approach to be used to generate projections and assess different possible control measures during future African swine fever virus outbreaks. This will help animal health policy makers optimise disease management decisions during future outbreaks.

Acknowledgments

The authors would like to acknowledge the coordinators of the African swine fever modelling challenge for developing this interesting modelling problem and for the opportunity to participate in the challenge.

Funding

This research did not receive any specific grant from funding agencies in the public, commercial, or not-for-profit sectors. E.A.D was funded by a Rhodes Scholarship and a studentship at the Department of Statistics, University of Oxford. S.L. was funded by the EDCTP program supported by the European Union (FibroScHot ref: RIA2017NIM-1842). S.H. was funded by the Engineering and Physical Sciences Research Council. C.A.D. was supported by joint Centre funding from the UK Medical Research Council and the UK Foreign, Commonwealth & Development Office (FCDO), under the MRC/FCDO Concordat agreement and is also part of the EDCTP2 programme supported by the European Union. C.A.D. was funded on grants from the UK National Institute for Health Research (NIHR) [Vaccine Efficacy Evaluation for Priority Emerging Diseases: PR-OD-1017-20007 and HPRU in Emerging and Zoonotic Infections: NIHR200907]. The views expressed in this publication are those of the authors and not necessarily those of their funding institutions.

Declarations of interest: none

CRediT author statement

Emmanuelle A. Dankwa: Conceptualization, Methodology, Formal analysis, Data Curation, Writing – Original Draft, Writing – Review & Editing, Visualization. **Sébastien Lambert**: Conceptualization, Methodology, Formal analysis, Data Curation, Writing – Original Draft, Writing – Review & Editing, Visualization. **Sarah Hayes**: Conceptualization, Methodology, Data Curation, Writing – Original Draft, Writing – Review & Editing. **Robin Thompson**: Conceptualization, Methodology, Writing – Original Draft, Writing – Review & Editing, Supervision. **Christl A. Donnelly**: Conceptualization, Methodology, Writing – Original Draft, Writing – Review & Editing, Supervision.

References

Altizer, S., Dobson, A., Hosseini, P., Hudson, P., Pascual, M., Rohani, P., 2006. Seasonality and the dynamics of infectious diseases. Ecol Lett 9, 467–484. https://doi.org/10.1111/j.1461-0248.2005.00879.x

Alves da Silva, A., Santos, P., Bento, P., Alves, J., Soares, A., Fonseca, C., Petrucci-Fonseca, F., Monzón, A., Silvério, A., 2004. Reproduction in the wild boar (Sus scrofa Linnaeus, 1758) populations of Portugal. Galemys 16, 53–65.

Andraud, M., Halasa, T., Boklund, A., Rose, N., 2019. Threat to the French swine industry of African swine fever: surveillance, spread, and control perspectives. Front Vet Sci 6, 248. https://doi.org/10.3389/fvets.2019.00248

Barongo, M.B., Bishop, R.P., Fèvre, E.M., Knobel, D.L., Ssematimba, A., 2016. A mathematical model that simulates control options for African swine fever virus (ASFV). PLoS One 11, e0158658. https://doi.org/10.1371/journal.pone.0158658

Barongo, M.B., Ståhl, K., Bett, B., Bishop, R.P., Fèvre, E.M., Aliro, T., Okoth, E., Masembe, C., Knobel, D., Ssematimba, A., 2015. Estimating the basic reproductive number (R0) for African Swine Fever Virus (ASFV) transmission between pig herds in Uganda. PLoS One 10, e0125842. https://doi.org/10.1371/journal.pone.0125842

Beaumont, M.A., Zhang, W., Balding, D.J., 2002. Approximate Bayesian computation in population genetics. Genetics 162, 2025–2035.

Beltrán-Alcrudo, D., Lubroth, J., Depner, K., De La Rocque, S., 2008. African swine fever in the Caucasus. FAO Empres Watch 1, 1–8.

Blome, S., Franzke, K., Beer, M., 2020. African swine fever – A review of current knowledge. Virus Res 287, 198099. https://doi.org/10.1016/j.virusres.2020.198099

Blome, S., Gabriel, C., Beer, M., 2013. Pathogenesis of African swine fever in domestic pigs and European wild boar. Virus Res 173, 122–130. https://doi.org/10.1016/j.virusres.2012.10.026

Blome, S., Gabriel, C., Dietze, K., Breithaupt, A., Beer, M., 2012. High virulence of African swine fever virus caucasus isolate in European wild boars of all ages. Emerg Infect Dis 18, 708. https://doi.org/10.3201/eid1804.111813

Brooks-Pollock, E., Roberts, G.O., Keeling, M.J., 2014. A dynamic model of bovine tuberculosis spread and control in Great Britain. Nature 511, 228–231. https://doi.org/10.1038/nature13529

Chenais, E., Depner, K., Guberti, V., Dietze, K., Viltrop, A., Ståhl, K., 2019. Epidemiological considerations on African swine fever in Europe 2014–2018. Porc. Health Manag. 5, 1–10.

Chenais, E., Ståhl, K., Guberti, V., Depner, K., 2018. Identification of wild boar-habitat epidemiologic cycle in African swine fever epizootic. Emerg Infect Dis 24, 810–812. https://doi.org/10.3201/eid2404.172127

Costard, S., Mur, L., Lubroth, J., Sanchez-Vizcaino, J.M., Pfeiffer, D.U., 2013. Epidemiology of African swine fever virus. Virus Res 173, 191–197. https://doi.org/10.1016/j.virusres.2012.10.030

Croft, S., Massei, G., Smith, G.C., Fouracre, D., Aegerter, J.N., 2020. Modelling spatial and temporal patterns of African swine fever in an isolated wild boar population to support decision-making. Front Vet Sci 7, 154. https://doi.org/10.3389/fvets.2020.00154

Danzetta, M.L., Marenzoni, M.L., Iannetti, S., Tizzani, P., Calistri, P., Feliziani, F., 2020. African swine fever: Lessons to learn from past eradication experiences. A systematic review. Front Vet Sci 7, 296. https://doi.org/10.3389/fvets.2020.00296

de Carvalho Ferreira, H.C., Backer, J.A., Weesendorp, E., Klinkenberg, D., Stegeman, J.A., Loeffen, W.L.A., 2013. Transmission rate of African swine fever virus under experimental conditions. Vet Microbiol 165, 296–304. https://doi.org/10.1016/j.vetmic.2013.03.026

Dellicour, S., Desmecht, D., Paternostre, J., Malengreaux, C., Licoppe, A., Gilbert, M., Linden, A., 2020. Unravelling the dispersal dynamics and ecological drivers of the African swine fever outbreak in Belgium. J Appl Ecol 57, 1619–1629. https://doi.org/10.1111/1365-2664.13649

Dixon, L.K., Sun, H., Roberts, H., 2019. African swine fever. Antivir. Res 165, 34–41. https://doi.org/10.1016/j.antiviral.2019.02.018

European Commission, 2020a. Commission Delegated Regulation (EU) 2020/687 of 17 December 2019 supplementing Regulation (EU) 2016/429 of the European Parliament and the Council, as regards rules for the prevention and control of certain listed diseases. J Eur Union L 174, 64–139.

European Commission, 2020b. Strategic approach to the management of African Swine Fever for the EU (Working Document No. SANTE/7113/2015 – Rev 12), Directorate G - Crisis management in food, animals and plants Unit G3 – Official controls and eradication of diseases in animals. Brussels.

European Commission, 2016. Regulation on transmissible animal diseases and amending and repealing certain acts in the area of animal health ('Animal Health Law'). J Eur Union L 84, 1–208.

European Commission, 2002. Proposal for a Council Directive laying down specific provisions for the control of African swine fever and amending Directive 92/119/EEC as regards Teschen disease and African swine fever (COM(2002)51 final). J Eur Union 181 E, 0142—0159.

European Food Safety Authority, 2015. Scientific opinion on African swine fever. EFSA J 13, 4163. https://doi.org/10.2903/j.efsa.2015.4163

European Food Safety Authority, Boklund, A., Cay, B., Depner, K., Földi, Z., Guberti, V., Masiulis, M., Miteva, A., More, S., Olsevskis, E., others, 2018. Epidemiological analyses of African swine fever in the European Union (November 2017 until November 2018). EFSA J 16, 5494. https://doi.org/10.2903/j.efsa.2018.5494

European Food Safety Authority, Desmecht, D., Gerbier, G., Gortázar Schmidt, C., Grigaliuniene, V., Helyes, G., Kantere, M., Korytarova, D., Linden, A., Miteva, A., others, 2021. Epidemiological analysis of African swine fever in the European Union (September 2019 to August 2020). EFSA J 19, 6572. https://doi.org/10.2903/j.efsa.2021.6572

Fischer, M., Hühr, J., Blome, S., Conraths, F.J., Probst, C., 2020. Stability of African swine fever virus in carcasses of domestic pigs and wild boar experimentally infected with the ASFV "Estonia 2014" isolate. Viruses 12, 1118. https://doi.org/10.3390/V12101118

Gallardo, C., Soler, A., Nieto, R., Cano, C., Pelayo, V., Sánchez, M.A., Pridotkas, G., Fernandez-Pinero, J., Briones, V., Arias, M., 2017. Experimental infection of domestic pigs with African swine fever virus Lithuania 2014 genotype II field isolate. Transbound Emerg Dis 64, 300–304. https://doi.org/10.1111/tbed.12346

Gervasi, V., Guberti, V., 2021. African swine fever endemic persistence in wild boar populations: Key mechanisms explored through modelling. Transbound Emerg Dis 68, 2812–2825. https://doi.org/10.1111/tbed.14194

Gervasi, V., Marcon, A., Bellini, S., Guberti, V., 2020. Evaluation of the efficiency of active and passive surveillance in the detection of African swine fever in wild boar. Vet Sci 7, 5. https://doi.org/10.3390/vetsci7010005

Global Framework for the Progressive Control of Transboundary Animal Diseases, 2020. Expert mission on African Swine Fever in Belgium Report.

Gogin, A., Gerasimov, V., Malogolovkin, A., Kolbasov, D., 2013. African swine fever in the North Caucasus region and the Russian Federation in years 2007-2012. Virus Res 173, 198–203. https://doi.org/10.1016/j.virusres.2012.12.007

Gonzales, W., Moreno, C., Duran, U., Henao, N., Bencosme, M., Lora, P., Reyes, R., Núñez, R., De Gracia, A., Perez, A.M., 2021. African swine fever in the Dominican Republic. Transbound. Emerg. Dis. 68, 3018–3019.

Guinat, C., Gogin, A., Blome, S., Keil, G., Pollin, R., Pfeiffer, D.U., Dixon, L., 2016a. Transmission routes of African swine fever virus to domestic pigs: Current knowledge and future research directions. Vet Rec. https://doi.org/10.1136/vr.103593

Guinat, C., Gubbins, S., Vergne, T., Gonzales, J.L., Dixon, L., Pfeiffer, D.U., 2016b. Experimental pig-to-pig transmission dynamics for African swine fever virus, Georgia 2007/1 strain. Epidemiol Infect 144, 25–34. https://doi.org/10.1017/S0950268815000862

Guinat, C., Porphyre, T., Gogin, A., Dixon, L., Pfeiffer, D.U., Gubbins, S., 2018. Inferring within-herd transmission parameters for African swine fever virus using mortality data from outbreaks in the Russian Federation. Transbound Emerg Dis 65, e264–e271. https://doi.org/10.1111/tbed.12748

Gulenkin, V.M., Korennoy, F.I., Karaulov, A.K., Dudnikov, S.A., 2011. Cartographical analysis of African swine fever outbreaks in the territory of the Russian Federation and computer modeling of the basic reproduction ratio. Prev Vet Med 102, 167–174. https://doi.org/10.1016/j.prevetmed.2011.07.004

Halasa, T., Boklund, A., Bøtner, A., Mortensen, S., Kjær, L.J., 2019. Simulation of transmission and persistence of African swine fever in wild boar in Denmark. Prev Vet Med 167, 68–79. https://doi.org/10.1016/j.prevetmed.2019.03.028

Halasa, T., Boklund, A., Bøtner, A., Toft, N., Thulke, H.-H., 2016a. Simulation of spread of African swine fever, including the effects of residues from dead animals. Front Vet Sci 3, 6. https://doi.org/10.3389/fvets.2016.00006

Halasa, T., Bøtner, A., Mortensen, S., Christensen, H., Toft, N., Boklund, A., 2016b. Control of African swine fever epidemics in industrialized swine populations. Vet Microbiol 197, 142–150. https://doi.org/10.1016/j.vetmic.2016.11.023

Halasa, T., Bøtner, A., Mortensen, S., Christensen, H., Toft, N., Boklund, A., 2016c. Simulating the epidemiological and economic effects of an African swine fever epidemic in industrialized swine populations. Vet Microbiol 193, 7–16. https://doi.org/10.1016/j.vetmic.2016.08.004

Halasa, T., Bøtner, A., Mortensen, S., Christensen, H., Wulff, S.B., Boklund, A., 2018. Modeling the effects of duration and size of the control zones on the consequences of a hypothetical African swine fever epidemic in Denmark. Front Vet Sci 5, 49. https://doi.org/10.3389/fvets.2018.00049

Hayes, B.H., Andraud, M., Salazar, L.G., Rose, N., Vergne, T., 2021. Mechanistic modelling of African swine fever: A systematic review. Prev. Vet. Med. 191, 105358.

Herrero, J., García-Serrano, A., García-González, R., 2008. Reproductive and demographic parameters in two Iberian wild boar Sus scrofa populations. Mammal Res 53, 355–364. https://doi.org/10.1007/BF03195196

Hu, B., Gonzales, J.L., Gubbins, S., 2017. Bayesian inference of epidemiological parameters from transmission experiments. Sci Rep 7, 1–13. https://doi.org/10.1038/s41598-017-17174-8

International Society for Infectious Diseases, 2022. African swine fever - Europe (02): Italy (Piedmont) wild boar. ProMED-Mail Post Arch Number 202201108700778.

International Society for Infectious Diseases, 2021. African swine fever - Europe (15): Germany (BB) 1st report in domestic pig. ProMED-Mail Post Arch Number 202107168522973.

Janeau, G., Cargnelutti, B., Cousse, S., Hewison, M., Spitz, F., 1995. Daily movement pattern variations in wild boar (Sus scrofa L.). Ibex JME 3, 98–101.

Jezierski, W., 1977. Longevity and mortality rate in a population of wild boar. Acta Theriol. (Warsz.) 22, 337–348.

Jo, Y.-S., Gortázar, C., 2021. African swine fever in wild boar: Assessing interventions in South Korea. Transbound Emerg Dis 68, 2878–2889. https://doi.org/10.1111/TBED.14106

Johansson, M.A., Apfeldorf, K.M., Dobson, S., Devita, J., Buczak, A.L., Baugher, B., Moniz, L.J., Bagley, T., Babin, S.M., Guven, E., others, 2019. An open challenge to advance probabilistic forecasting for dengue epidemics. Proc Natl Acad Sci U A 116, 24268–24274.

Jori, F., Vial, L., Penrith, M.L., Pérez-Sánchez, R., Etter, E., Albina, E., Michaud, V., Roger, F., 2013. Review of the sylvatic cycle of African swine fever in sub-Saharan Africa and the Indian ocean. Virus Res 173, 212–227. https://doi.org/10.1016/j.virusres.2012.10.005

Keuling, O., Stier, N., Roth, M., 2008. Annual and seasonal space use of different age classes of female wild boar Sus scrofa L. Eur J Wildl Res 54, 403–412. https://doi.org/10.1007/s10344-007-0157-4

Lange, M., 2015. Alternative control strategies against ASF in wild boar populations. EFSA Support. Publ. 12, 843E.

Lange, M., Guberti, V., Thulke, H.-H., 2018. Understanding ASF spread and emergency control concepts in wild boar populations using individual-based modelling and spatio-temporal surveillance data. EFSA Support Publ 15, 1521E. https://doi.org/10.2903/sp.efsa.2018.en-1521

Lange, M., Thulke, H.-H., 2017. Elucidating transmission parameters of African swine fever through wild boar carcasses by combining spatio-temporal notification data and agent-based modelling. Stoch Env. Res Risk Assess 31, 379–391. https://doi.org/10.1007/s00477-016-1358-8

Lange, M., Thulke, H.-H., 2015. Mobile barriers as emergency measure to control outbreaks of African Swine Fever in wild boar, in: Proc. Annu. Meet. Soc. Vet. Epidemiol. Prev. Med. pp. 122–132.

Lee, H.S., Thakur, K.K., Bui, V.N., Pham, T.L., Bui, A.N., Dao, T.D., Thanh, V.T., Wieland, B., 2021. A stochastic simulation model of African swine fever transmission in domestic pig farms in the Red River Delta region in Vietnam. Transbound Emerg Dis 68, 1384–1391. https://doi.org/10.1111/tbed.13802

Loi, F., Cappai, S., Laddomada, A., Feliziani, F., Oggiano, A., Franzoni, G., Rolesu, S., Guberti, V., 2020. Mathematical approach to estimating the main epidemiological parameters of African swine fever in wild boar. Vaccines 8, 1–20. https://doi.org/10.3390/vaccines8030521

Luskin, M.S., Meijaard, E., Surya, S., Sheherazade, Walzer, C., Linkie, M., 2020. African swine fever threatens Southeast Asia's 11 endemic wild pig species. Conserv Lett 14, e12784. https://doi.org/10.1111/conl.12784

Marcon, A., Linden, A., Satran, P., Gervasi, V., Licoppe, A., Guberti, V., 2020. R0 estimation for the African swine fever epidemics in wild boar of Czech Republic and Belgium. Vet Sci 7, 2. https://doi.org/10.3390/vetsci7010002

Maselli, V., Rippa, D., Russo, G., Ligrone, R., Soppelsa, O., D'Aniello, B., Raia, P., Fulgione, D., 2014. Wild boars' social structure in the Mediterranean habitat. Ital J Zool 81, 610–617. https://doi.org/10.1080/11250003.2014.953220

Mauroy, A., Depoorter, P., Saegerman, C., Cay, B., De Regge, N., Filippitzi, M.-E., Fischer, C., Laitat, M., Maes, D., Morelle, K., others, 2021. Semi-quantitative risk assessment by expert elicitation of potential introduction routes of African swine fever from wild reservoir to domestic pig industry and subsequent spread during the Belgian outbreak (2018–2019). Transbound. Emerg. Dis. 68, 2761–2773.

Mazur-Panasiuk, N., Woźniakowski, G., 2020. Natural inactivation of African swine fever virus in tissues: Influence of temperature and environmental conditions on virus survival. Vet Microbiol 242, 108609. https://doi.org/10.1016/j.vetmic.2020.108609

McGowan, C.J., Biggerstaff, M., Johansson, M., Apfeldorf, K.M., Ben-Nun, M., Brooks, L., Convertino, M., Erraguntla, M., Farrow, D.C., Freeze, J., others, 2019. Collaborative efforts to forecast seasonal influenza in the United States, 2015–2016. Sci Rep 9, 1–13. https://doi.org/10.1038/s41598-018-36361-9

Mellor, P.S., Kitching, R.P., Wilkinson, P.J., 1987. Mechanical transmission of capripox virus and African swine fever virus by Stomoxys calcitrans. Res Vet Sci 43, 109–112. https://doi.org/10.1016/s0034-5288(18)30753-7

Mighell, E., Ward, M.P., 2021. African swine fever spread across Asia, 2018–2019. Transbound Emerg Dis 68, 2722–2732. https://doi.org/10.1111/tbed.14039

Minter, A., Retkute, R., 2019. Approximate Bayesian computation for infectious disease modelling. Epidemics 29, 100368. https://doi.org/10.1016/j.epidem.2019.100368

Miteva, A., Papanikolaou, A., Gogin, A., Boklund, A., Bøtner, A., Linden, A., Viltrop, A., Schmidt, C.G., Ivanciu, C., Desmecht, D., Korytarova, D., Olsevskis, E., Helyes, G., Wozniakowski, G., Thulke, H.H., Roberts, H., Abrahantes, J.C., Ståhl, K., Depner, K., González Villeta, L.C., Spiridon, M., Ostojic, S., More, S., Vasile, T.C., Grigaliuniene, V., Guberti, V., Wallo, R., 2020. Epidemiological analyses of African swine fever in the European Union (November 2018 to October 2019). EFSA J 18, 5996. https://doi.org/10.2903/j.efsa.2020.5996

Mulumba-Mfumu, L.K., Saegerman, C., Dixon, L.K., Madimba, K.C., Kazadi, E., Mukalakata, N.T., Oura, C.A.L., Chenais, E., Masembe, C., Ståhl, K., Thiry, E., Penrith, M.L., 2019. African swine fever: Update on Eastern, Central and Southern Africa. Transbound Emerg Dis. https://doi.org/10.1111/tbed.13187

Mur, L., Sánchez-Vizcaíno, J.M., Fernández-Carrión, E., Jurado, C., Rolesu, S., Feliziani, F., Laddomada, A., Martínez-López, B., 2018. Understanding African swine fever infection dynamics in Sardinia using a spatially explicit transmission model in domestic pig farms. Transbound Emerg Dis 65, 123–134. https://doi.org/10.1111/tbed.12636

Nielsen, J.P., Larsen, T.S., Halasa, T., Christiansen, L.E., 2017. Estimation of the transmission dynamics of African swine fever virus within a swine house. Epidemiol Infect 145, 2787–2796. https://doi.org/10.1017/S0950268817001613

Oganesyan, A.S., Petrova, O.N., Korennoy, F.I., Bardina, N.S., Gogin, A.E., Dudnikov, S.A., 2013. African swine fever in the Russian Federation: spatio-temporal analysis and epidemiological overview. Virus Res 173, 204–211. https://doi.org/10.1016/j.virusres.2012.12.009

Olesen, A.S., Lohse, L., Hansen, M.F., Boklund, A., Halasa, T., Belsham, G.J., Rasmussen, T.B., Bøtner, A., Bødker, R., 2018. Infection of pigs with African swine fever virus via ingestion of stable flies (Stomoxys calcitrans). Transbound Emerg Dis 65, 1152–1157. https://doi.org/10.1111/tbed.12918

O'Neill, X., White, A., Ruiz-Fons, F., Gortázar, C., 2020. Modelling the transmission and persistence of African swine fever in wild boar in contrasting European scenarios. Sci Rep. 2020 101 10, 1–10. https://doi.org/10.1038/s41598-020-62736-y

Penrith, M.L., Bastos, A.D., Etter, E.M.C., Beltrán-Alcrudo, D., 2019. Epidemiology of African swine fever in Africa today: Sylvatic cycle versus socio-economic imperatives. Transbound Emerg Dis 66, 672–686. https://doi.org/10.1111/tbed.13117

Pepin, K.M., Golnar, A., Podgórski, T., 2021. Social structure defines spatial transmission of African swine fever in wild boar. J R Soc Interface 18, 20200761. https://doi.org/10.1098/RSIF.2020.0761

Pepin, K.M., Golnar, A.J., Abdo, Z., Podgórski, T., 2020. Ecological drivers of African swine fever virus persistence in wild boar populations: Insight for control. Ecol Evol 10, 2846–2859. https://doi.org/10.1002/ece3.6100

Picault, S., Vergne, T., Mancini, M., Bareille, S., Ezanno, P., 2021. The African swine fever modelling challenge: objectives, model description and synthetic data generation. bioRxiv 2021.12.20.473417. https://doi.org/10.1101/2021.12.20.473417

Pietschmann, J., Guinat, C., Beer, M., Pronin, V., Tauscher, K., Petrov, A., Keil, G., Blome, S., 2015. Course and transmission characteristics of oral low-dose infection of domestic pigs and European wild boar with a Caucasian African swine fever virus isolate. Arch Virol 160, 1657–1667. https://doi.org/10.1007/s00705-015-2430-2

Podgórski, T., Baś, G., Jędrzejewska, B., Sönnichsen, L., Śnieżko, S., Jędrzejewski, W., Okarma, H., 2013. Spatiotemporal behavioral plasticity of wild boar (Sus scrofa) under contrasting conditions of human pressure: primeval forest and metropolitan area. J. Mammal. 94, 109–119.

Podgórski, T., Lusseau, D., Scandura, M., Sönnichsen, L., Jędrzejewska, B., 2014. Long-lasting, kin-directed female interactions in a spatially structured wild boar social network. PLoS One 9, e99875.

Podgórski, T., Śmietanka, K., 2018. Do wild boar movements drive the spread of African swine fever? Transbound Emerg Dis 65, 1588–1596. https://doi.org/10.1111/tbed.12910

Pollock, L.A., Newton, E.J., Koen, E.L., 2021. Predicting high-risk areas for African swine fever spread at the wild-domestic pig interface in Ontario. Prev. Vet. Med. 191, 105341.

Probst, C., Globig, A., Knoll, B., Conraths, F.J., Depner, K., 2017. Behaviour of free ranging wild boar towards their dead fellows: Potential implications for the transmission of African swine fever. R Soc Open Sci 4. https://doi.org/10.1098/rsos.170054

R Core Team, 2022. R: A language and environment for statistical computing. R Foundation for Statistical Computing, Vienna, Austria.

Reich, N.G., McGowan, C., Yamana, T., Tushar, A., Ray, E., Osthus, D., Kandula, S., Brooks, L.C., Crawford-Crudell, W., Gibson, G.C., others, 2019. Accuracy of real-time multi-model ensemble forecasts for seasonal influenza in the U.S. PLoS Comput Biol 15, e1007486. https://doi.org/10.1371/JOURNAL.PCBI.1007486

Relun, A., Grosbois, V., Alexandrov, T., Sánchez-Vizcaíno, J.M., Waret-Szkuta, A., Molia, S., Charles Etter, E.M., Martínez-López, B., 2017. Prediction of pig trade movements in different European production systems using exponential random graph models. Front Vet Sci 4, 27. https://doi.org/10.3389/fvets.2017.00027

Rosell, C., Navàs, F., Romero, S., 2012. Reproduction of wild boar in a cropland and coastal wetland area: implications for management. Anim Biodivers Conserv 35, 209–217. https://doi.org/10.32800/abc.2012.35.0209

Rowlands, R.J., Michaud, V., Heath, L., Hutchings, G., Oura, C., Vosloo, W., Dwarka, R., Onashvili, T., Albina, E., Dixon, L.K., 2008. African swine fever virus isolate, Georgia, 2007. Emerg Infect Dis 14, 1870–1874. https://doi.org/10.3201/eid1412.080591

Sabrina, S., Jean-Michel, G., Carole, T., Serge, B., Eric, B., 2009. Pulsed resources and climate-induced variation in the reproductive traits of wild boar under high hunting pressure. J Anim Ecol 78, 1278–1290. https://doi.org/10.1111/j.1365-2656.2009.01579.x

Saltelli, A., Ratto, M., Andres, T., Campolongo, F., Cariboni, J., Gatelli, D., Saisana, M., Tarantola, S., 2008. Global sensitivity analysis. The primer. John Wiley & Sons.

Sánchez-Cordón, P.J., Nunez, A., Neimanis, A., Wikström-Lassa, E., Montoya, M., Crooke, H., Gavier-Widén, D., 2019. African swine fever: Disease dynamics in wild boar experimentally infected with ASFV isolates belonging to genotype I and II. Viruses 11, 852. https://doi.org/10.3390/v11090852

Sauter-Louis, C., Forth, J.H., Probst, C., Staubach, C., Hlinak, A., Rudovsky, A., Holland, D., Schlieben, P., Göldner, M., Schatz, J., others, 2021a. Joining the club: First detection of African swine fever in wild boar in Germany. Transbound Emerg Dis 68, 1744–1752. https://doi.org/10.1111/tbed.13890

Sauter-Louis, C., Schulz, K., Richter, M., Staubach, C., Mettenleiter, T.C., Conraths, F.J., 2021b. African swine fever: Why the situation in Germany is not comparable to that in the Czech Republic or Belgium. Transbound. Emerg. Dis.

Shi, R., Li, Y., Wang, C., 2020. Stability analysis and optimal control of a fractional-order model for African swine fever. Virus Res 288, 198111. https://doi.org/10.1016/j.virusres.2020.198111

Taylor, R.A., Podgórski, T., Simons, R.R., Ip, S., Gale, P., Kelly, L.A., Snary, E.L., 2021. Predicting spread and effective control measures for African swine fever—Should we blame the boars? Transbound. Emerg. Dis. 68, 397–416.

Thulke, H.-H., Lange, M., 2017. Simulation-based investigation of ASF spread and control in wildlife without consideration of human non-compliance to biosecurity. EFSA Support Publ 14, 1312E. https://doi.org/10.2903/sp.efsa.2017.en-1312

Tian, X., von Cramon-Taubadel, S., 2020. Economic consequences of African swine fever. Nat Food 1, 196–197. https://doi.org/10.1038/s43016-020-0061-6

Toni, T., Welch, D., Strelkowa, N., Ipsen, A., Stumpf, M.P., 2009. Approximate Bayesian computation scheme for parameter inference and model selection in dynamical systems. J R Soc Interface 6, 187–202.

U.S. Department of Agriculture, 2021. USDA Statement on Confirmation of African Swine Fever in Haiti [WWW Document]. URL https://www.aphis.usda.gov/aphis/newsroom/stakeholder-info/sa_by_date/sa-2021/sa-09/asf-haiti (accessed 6.23.22).

Vergne, T., Andraud, M., Bonnet, S., De Regge, N., Desquesnes, M., Fite, J., Etore, F., Garigliany, M.M., Jori, F., Lempereur, L., others, 2021. Mechanical transmission of African swine fever virus by Stomoxys calcitrans: Insights from a mechanistic model. Transbound Emerg Dis 68, 1541–1549. https://doi.org/10.1111/tbed.13824

Viboud, C., Sun, K., Gaffey, R., Ajelli, M., Fumanelli, L., Merler, S., Zhang, Q., Chowell, G., Simonsen, L., Vespignani, A., others, 2018. The RAPIDD Ebola forecasting challenge: Synthesis and lessons learnt. Epidemics 22, 13–21.

Viltrop, A., Boinas, F., Depner, K., Jori, F., Kolbasov, D., Laddomada, A., Ståhl, K., Chenais, E., 2021. African swine fever epidemiology, surveillance and control, in: Underst. Combat. African Swine Fever A Eur. Perspect. Wageningen Academic Publishers, pp. 229–261. https://doi.org/10.3920/978-90-8686-910-7_9

World Organisation for Animal Health, 2022. African Swine Fever (ASF) – Situation report 10 (No. 10).

World Organisation for Animal Health, 2021. African swine fever [WWW Document]. URL https://www.oie.int/en/disease/african-swine-fever/ (accessed 7.16.21).

World Organisation for Animal Health, 2020. African Swine Fever (ASF).

Yoo, D.S., Kim, Y., Lee, E.S., Lim, J.S., Hong, S.K., Lee, I.S., Jung, C.S., Yoon, H.C., Wee, S.H., Pfeiffer, D.U., Fournié, G., 2021. Transmission dynamics of African swine fever virus, South Korea, 2019. Emerg. Infect. Dis. 27, 1909.

Tables

Table 51: Epidemiological parameters. For estimated parameters, mean values along with 95% credible intervals (CrI; in parentheses) are reported.

	Description	Mean value(s) (95% CrI)	Source(s)
Wild boar			
α	Scale parameter of dispersal kernel	Phase 1: 0.8225 km (0.8006-0.8800) Phase 2: 0.87 km Phase 3: 1 km	Estimated at phase 1 Fixed at phases 2 & 3
β	Overall infection rate	Phase 1: 0.0018 day^{-1} (0.0011-0.0028) Phase 2: 0.0077 day^{-1} (0.0069-0.0084) Phase 3: 0.0035 day^{-1} (0.0034-0.0036)	Estimated
	Time from infection to death	14 days	(Blome et al., 2012; Pietschmann et al., 2015)
	Infectious period for carcasses	90 days	(Fischer et al., 2020)
	ASFV-related mortality rate	100%	(Blome et al., 2013, 2012)
Additional parameters for phase 1 model			
r_1	Fraction of positive boar in a patch when day <28, averaged over all patches	0.16 (0.09-0.20)	Estimated*
r_2	Fraction of positive boar in a patch when day ≥38, averaged over all patches	0.25 (0.20-0.38)	Estimated*
d	Detection rate for positive boar	0.10	Assumed
Domestic pig herds			
β^{PH}	Transmission rate	0.60 day^{-1}	(Guinat et al., 2016b)
τ	Mean lifetime of ASF virus in residues from dead pigs	$1/\log(2)$ days	Adapted from: (Halasa et al., 2016a)
δ	Average duration of the pre-infectious period	$\mathrm{PERT}(3;4;5)$ days†	(Guinat et al., 2016b; Vergne et al., 2021)
ϕ	Average duration of the subclinical period	2 days	ASF Challenge coordinators
γ	Average duration of the infectious period	$\mathrm{PERT}(3;7;14)$ days†	(Guinat et al., 2016b; Vergne et al., 2021)
μ	Probability of pigs dying following infection	0.95	(Gallardo et al., 2017; Halasa et al., 2016a)
ρ	Transmission rate by local spread	0.005 km.day^{-1}	Adapted from: (Halasa et al., 2016c)

* This parameter was defined to be time-varying to reflect the spread of the infection (in the absence of disease management measures) as time progressed. For day ∈ [28, 37], the fraction of positive boar in a patch was given by: $r_1 + \frac{r_2 - r_1}{38-28} \times (\mathrm{day} - 28)$

† PERT distribution of parameters (minimum; mode; maximum)

Table 52: Differences between models across the three phases of the challenge. As the challenge progressed, the models had to be slightly adapted to account for new data and information provided by the challenge coordinators and/or to answer new questions.

	Phase 1	**Phase 2**	**Phase 3**
Explicit modelling of individual infected boar in a patch (and their locations)	No	Yes	Yes
Detection of infected wild boar	Yes (fixed rate)	Yes (through testing of hunted boar and active surveillance of boar carcasses)	Yes (through testing of hunted boar and active surveillance of boar carcasses)
Increased hunting pressure in fence and buffer zone	Yes (no buffer zone)	Yes	Yes
Permeability of the fence	No	No	Yes
Maximum infection range (MIR)	No	No	Yes (8 km)
Test of preventively culled pig herds	Not applicable	No	Yes
Delay before preventive culling	Not applicable	Yes (24 hours)	Yes (5-7 days)

Table 53: Model fit and projections for the cumulative number of detected infections under the two main disease management scenarios considered in wild boar: increased hunting pressure and normal hunting pressure. The model fits are median model estimates for the observed period (days 1-50 for phase 1, days 1-80 for phase 2 and days 1-110 for phase 3) while the model projections are median model estimates for the unobserved periods over which projections were computed (days 51-78 for phase 1, days 81-110 for phase 2, days 111-230 for phase 3). Model estimates are medians of 500 simulations along with 95% credible intervals (CrI) in parentheses.

Phase	By day	Disease management scenario*	Wild boar			Pig herd		
			Observed	Model fit (95% CrI)	Model projections (95% CrI)	Observed	Model fit (95% CrI)	Model projections (95% CrI)
1	50		397	396 (358-435)		3	4 (2-6)	
	78	Increased hunting pressure			1770 (1445-2503)			8 (5-14)
		Normal hunting pressure			933 (751-1289)			8 (5-14)
2	80		2007	2009 (1912-2102)		12	12 (8-17)	
	110	Increased hunting pressure			3214 (3112-3378)			28 (22-35)
		Normal hunting pressure			3272 (2973-3868)			30 (23-38)
3	110		2984	2994 (2897-3077)		26	25 (21-31)	
	140	Increased hunting pressure			3442 (3372-3514)			38 (32-48)
		Normal hunting pressure			7954 (6891-8827)			87 (67-100)
	230	Increased hunting pressure			4599 (4480-4711)			113 (99-129)

* For all phases, scenarios are only indicated for projected periods and not for observed periods. For the observed periods, the scenario for phase 1 is normal hunting pressure with no fence whereas the scenario for phases 2 and 3 is increased hunting pressure.

Table 54: Comparison of model projections and observed (synthetic) data on the cumulative number of detected infected wild boar and pig herds up to days 78 and 110. For both wild boar and pig herds, model projections shown here assumed disease management measures as implemented during the indicated periods. Model estimates are medians of 500 simulations along with 95% credible intervals in parentheses.

Population	**Category**	**Cumulative number of detected infections up to:**	
		Day 78	**Day 110**
Wild boar	Model	1770 (1445-2503)	3214 (3112-3378)
	Observed	1903	2984
Pig herds	Model	8 (5-14)	31 (23-39)[1]
	Observed	10	26

[1] To adequately compare the results of the model with the synthetic data, the projections for pig herds up to day 110 (phase 2 model) were simulated using disease management measures as implemented during the indicated period, i.e., incorporating preventive culling of all pig herds located at less than 3 km from positive wild boar carcasses from day 90, with a delay of 5-7 days between the confirmation of a wild boar case and pig herd culling, and performing tests in all culled herds which provided results the day after.

Table 55: Number of detected infections in wild boar and pig herds by day 110 under alternative parameter values tested in the sensitivity analysis. Estimates presented are medians and 95% credible intervals (CrI) of 100 stochastic repetitions of the model. Parameter values as used in the baseline model (maximum infection range = 8 km, α = 1 km, duration of infectiousness in carcasses = 90 days; and duration of infectiousness in live boar = 14 days) and corresponding outcomes are in bold.

Parameter	**Values**	**Median number of detected infections by day 110 (95% CrI)**	
		Wild boar	**Pig herds**
Maximum infection range (km)	2	1435 (1395-1476)	12 (10-16)
	8	**2991 (2856-3125)**	**24 (20-29)**
	14	3043 (2891-3199)	24 (21-31)
	20	3061 (2924-3189)	24 (20-30)
Scale parameter of dispersal kernel, α (km)	0.6	1804 (1736-1861)	14 (11-19)
	0.8	2282 (2202-2361)	17 (14-21)
	1.0	**2991 (2856-3125)**	**24 (20-29)**
	1.2	4094 (3945-4279)	33 (28-40)
Duration of infectiousness in carcass (in days)	10	2756 (2639-2890)	23 (19-28)
	50	2995 (2868-3106)	24 (20-30)
	90	**2991 (2856-3125)**	**24 (20-29)**
	130	2982 (2835-3103)	24 (20-30)
Duration of infectiousness in live boar (in days)	5	2071 (1986-2138)	24 (20-29)
	7	2308 (2224-2434)	24 (20-29)
	10	2638 (2501-2774)	24 (20-28)
	14	**2991 (2856-3125)**	**24 (20-29)**

Table 6: Number of detected infections in wild boar and pig herds by day 140 under alternative intervention efficacies between day 111 and 140. Estimates presented are medians and 95% credible intervals (CrI) of 100 stochastic repetitions of the model.

Parameter value relative to baseline			Median number of detected infections by day 140 (95% CrI)	
Fence[1]	**Wild boar testing[2]**	**cullWB[3]**	**Wild boar**	**Pig herds**
100%	100%	100%	3443 (3323-3547)	38 (31-45)
		75%		37 (30-45)
		50%		37 (30-45)
	75%	100%	3407 (3297-3507)	39 (31-45)
		75%		38 (31-45)
		50%		37 (32-45)
	50%	100%	3361 (3252-3456)	38 (32-47)
		75%		37 (31-45)
		50%		37 (31-45)
75%	100%	100%	3443 (3338-3550)	38 (31-47)
		75%		38 (31-44)
		50%		38 (31-44)
	75%	100%	3400 (3299-3501)	39 (32-46)
		75%		37 (31-46)
		50%		37 (32-46)
	50%	100%	3369 (3278-3479)	39 (32-46)
		75%		38 (31-44)
		50%		38 (31-43)
50%	100%	100%	3444 (3344-3561)	39 (32-47)
		75%		38 (31-46)
		50%		38 (31-46)
	75%	100%	3408 (3312-3517)	39 (32-45)
		75%		38 (31-46)
		50%		38 (31-46)
	50%	100%	3372 (3273-3471)	39 (33-47)
		75%		38 (31-45)
		50%		39 (31-45)

[1] During phase 3, we allowed for a "leaky" fence in all directions, such that ASFV could be transmitted between two patches on opposite sides of the fence depending on the distance between their centres. Here, we tested different values of the efficacy of the fence when the maximum transmission distance for two patches i and j on opposite sides of the fence is equal to: $4\ \mathrm{km} = \mathrm{MIR}/2$ (baseline; 100%), $5.3\ \mathrm{km} = \mathrm{MIR}/(2 \times 0.75)$ (75%), or $8\ \mathrm{km} = \mathrm{MIR}/(2 \times 0.5)$ (50%).

[2] We evaluated three scenarios where a smaller fraction (compared to our baseline scenario) of wild boar were tested post-removal: 100% (baseline), 75% or 50%.

[3] Similarly, we evaluated three scenarios where only a fraction of pig herds located less than 3 km away from positive wild boar were culled: 100% (baseline), 75% or 50%.

Figures

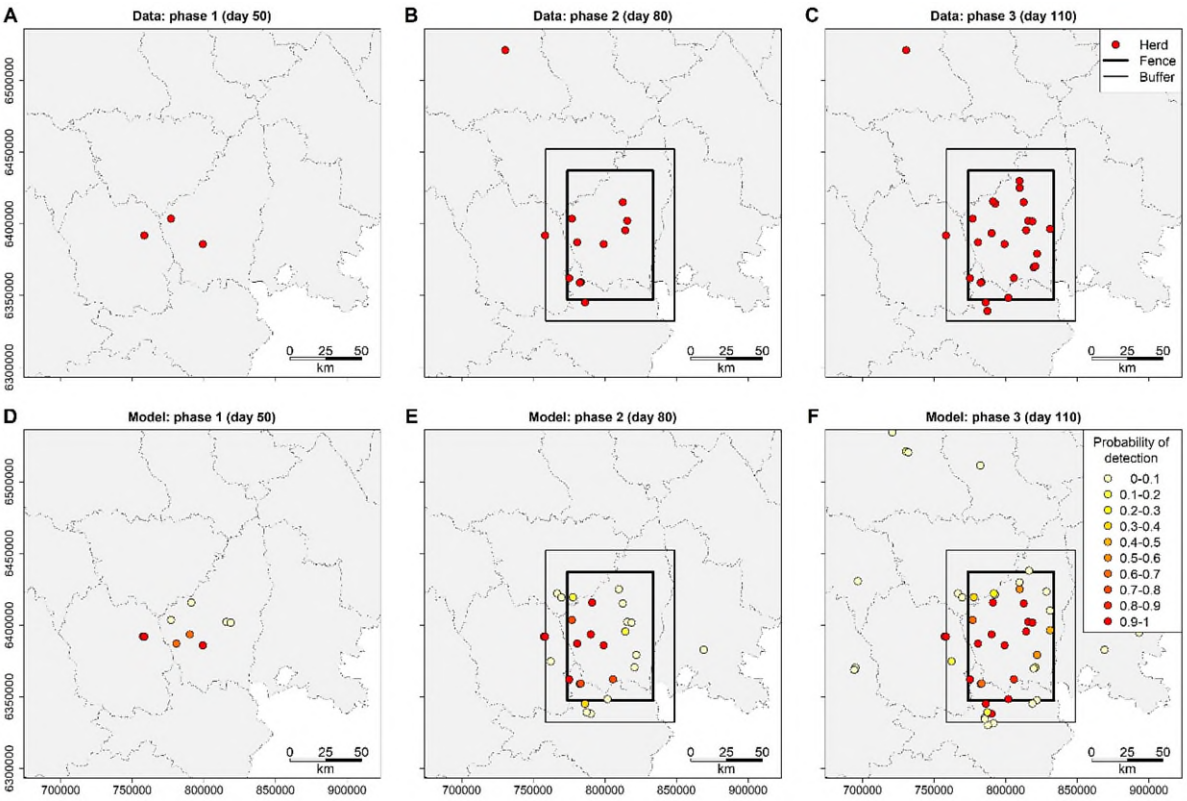

Figure 51: Distribution of detected infected pig herds on Merry Island: comparison between data (top panels showing only detected infected pig herds) and model simulations (bottom panels showing all pig herds that were detected as positive in at least one simulation) for each phase. **Top panels (A-C)**: detected herds by (A) day 50, (B) day 80 and (C) day 110 (for phase 1, 2 and 3 respectively) in the data provided by the challenge coordinators. Detected herds are indicated by red dots, while the fence and buffer zones (implemented during phases 2 and 3) are indicated by thick and thin rectangles, respectively. **Bottom panels (D-F)**: detected herds by (D) day 50, (E) day 80 and (F) day 110 in the model simulations run with estimated parameter values. Dots indicate herds that were detected in at least one simulation, with colours indicating the proportion of simulations in which a given herd was detected (among 500 simulations).

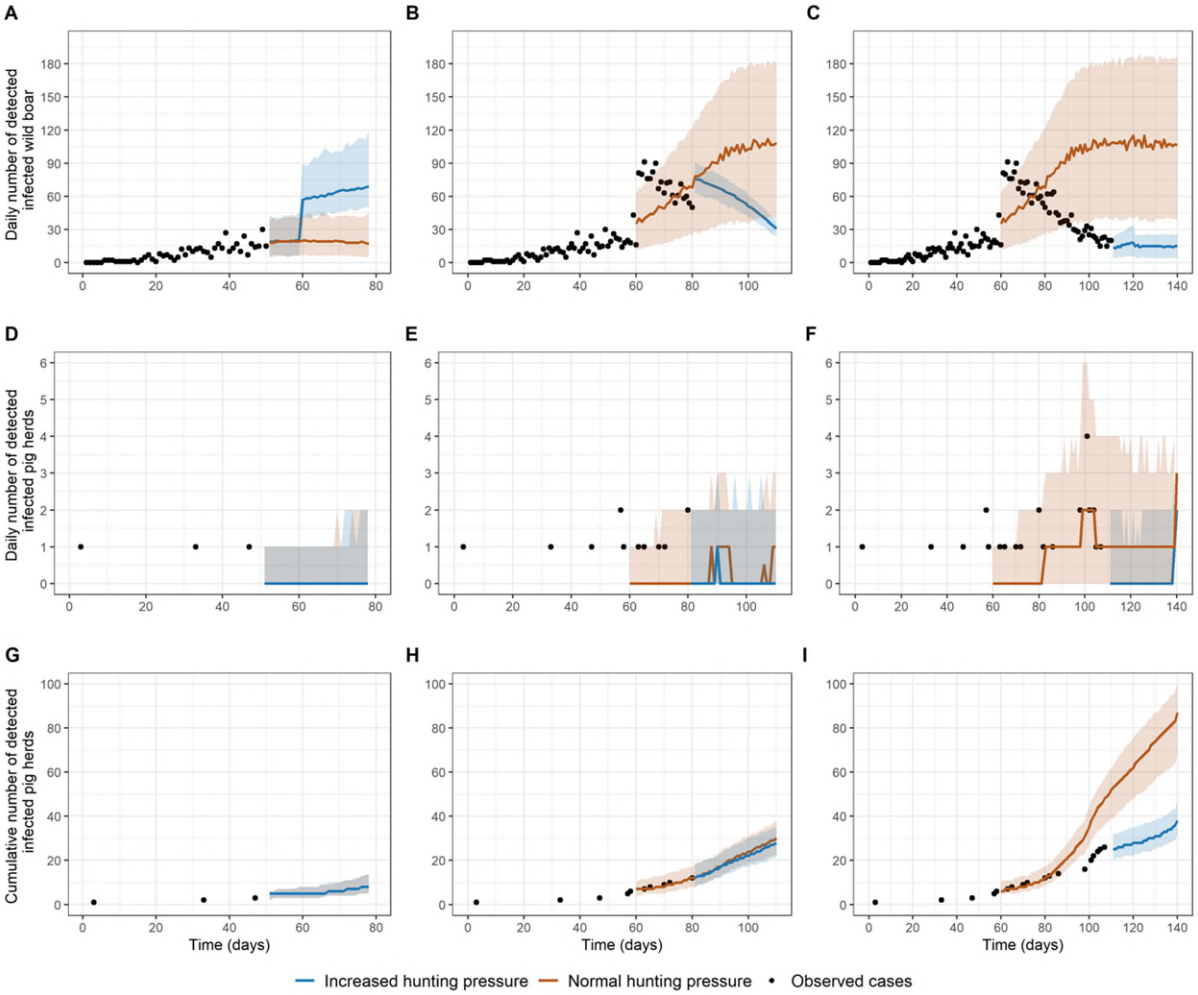

Figure 52: Comparison of disease management scenarios for wild boar (increased hunting pressure and normal hunting pressure) across all phases. **Top panels (A-C)**: Observed (black dots) and projected daily number of detected infected wild boar under the increased hunting pressure (blue) and normal hunting pressure (light orange) scenarios. In panel C, the drop at day 120 is due to a cessation in increased hunting pressure activities. **Middle panels (D-F)**: Observed (black dots) and projected daily number of detected infected pig herds under the increased hunting pressure (blue) and normal hunting pressure (light orange) scenarios. **Bottom panels (G-I)**: Observed (black dots) and resulting cumulative numbers of detected infected pig herds from the daily projections (D-F), under the increased hunting pressure (blue) and normal hunting pressure (light orange) scenarios. **All panels**: Median model projections are shown along with 95% credible intervals (shaded areas with corresponding colours). Projections were obtained using the model calibrated to data up to days 50, 80 and 110 for the increased hunting pressure scenario in Phase 1 (A, D, G), phase 2 (B, E, H) and phase 3 (C, F, I) respectively. For the normal hunting pressure scenario, the model was calibrated using data up to day 50 for phase 1 and up to day 59 for phases 2 and 3. **[Note: the observed data in all cases arose in the challenge scenario in which hunting pressure increased from day 60, making these data not directly comparable with the normal-hunting-pressure-throughout projections (light orange) in the middle and right-hand columns.]**

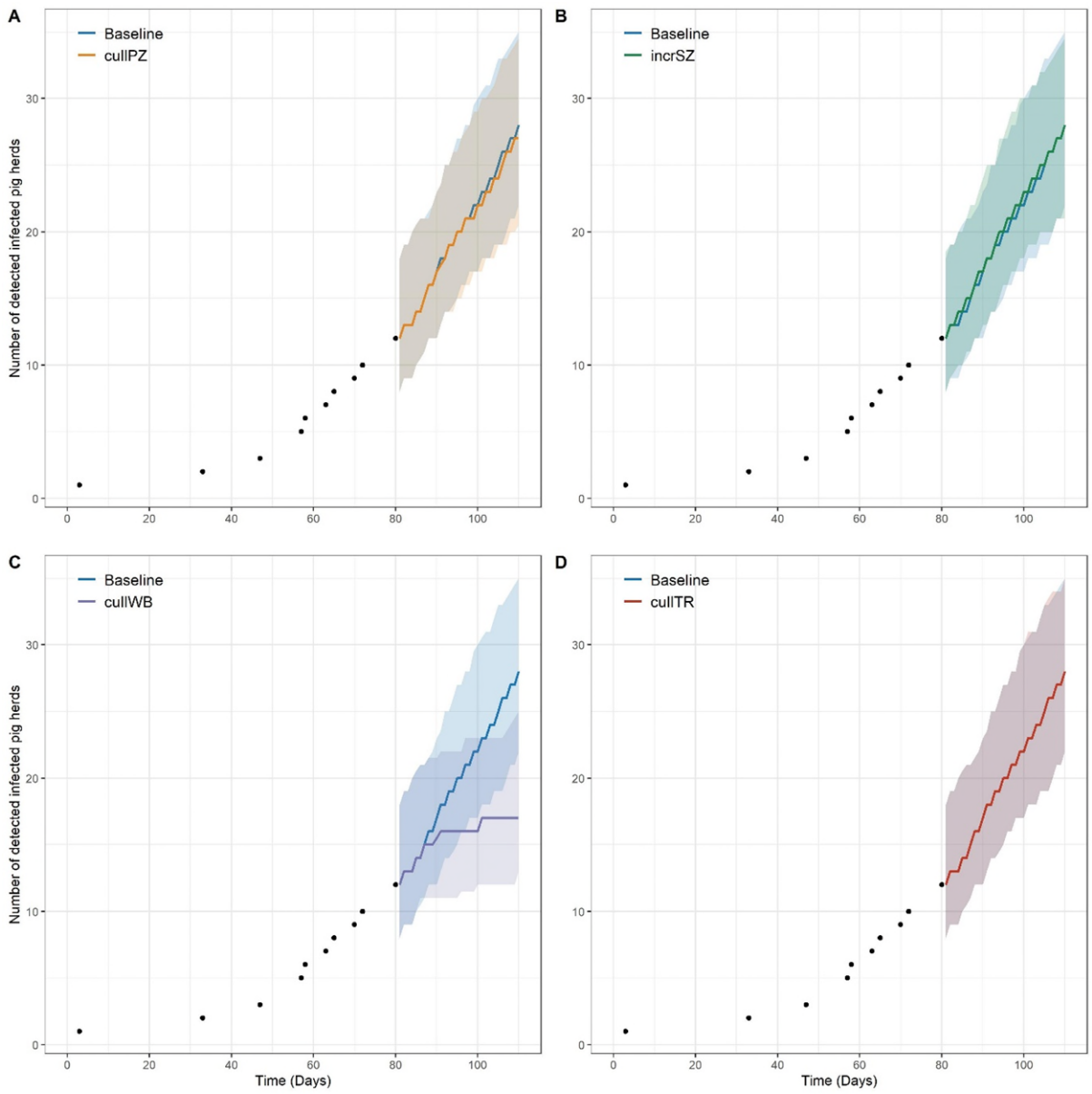

Figure 53: Comparison of the impact of additional disease management measures on the number of detected infected pig herds (phase 2). Median model projections are shown along with 95% credible intervals (shaded areas with corresponding colours), for a baseline scenario and four additional disease management measures implemented in pig herds. The baseline scenario ("Baseline") involved regulatory interventions in pig herds and the implementation of fencing and increased hunting pressure in wild boar. The four disease management measures implemented in addition to the baseline scenario are: (1) "cullPZ": culling of all pig herds in protection zones; (2) "incrSZ": increasing the size of the surveillance zone from 10 km (the standard surveillance radius used) to 15 km; (3) "cullWB": culling of all pig herds located at less than 3 km from positive wild boar; (4) "cullTR": culling of all herds that have traded pigs with an infected farm less than three weeks before detection.

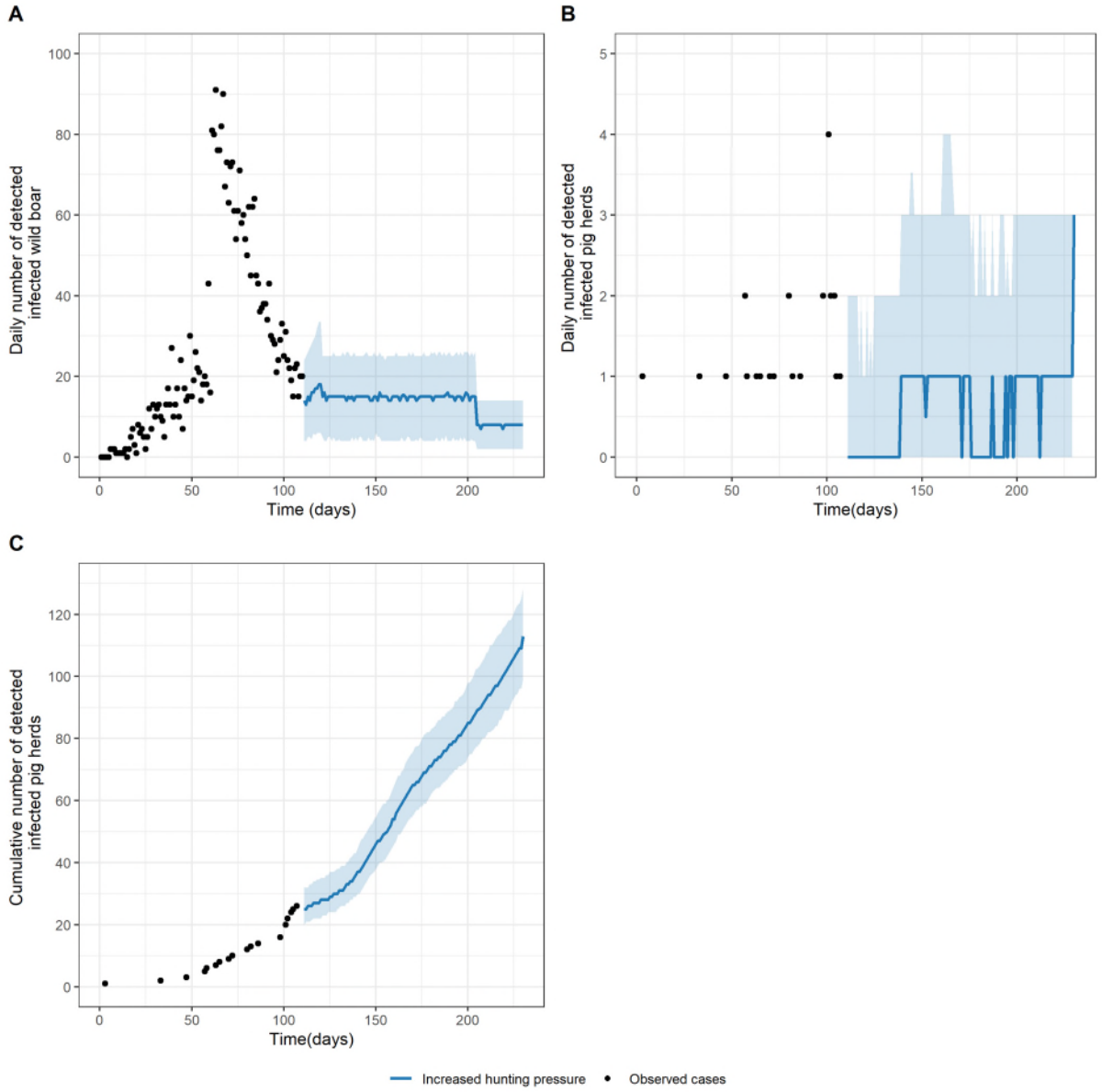

Figure 54: Model projections from day 111 to day 230 under the increased hunting pressure scenario. **A.** Observed and projected daily numbers of detected infected wild boar. Projections were obtained using the disease management measures as implemented over the indicated period: (1) increased hunting pressure from day 111 to day 120, (2) normal hunting pressure from day 121 to day 203 and (3) cessation in hunting activities (end of the hunting season) from day 204 onwards but permitting passive discovery of wild boar carcasses. The drop at day 204 is due to the cessation in hunting activities. **B.** Observed and projected daily numbers of detected infected pig herds. **C.** Observed and projected cumulative numbers of detected infected pig herds. **All**: Black dots, blue line and shaded areas represent the observed data, median model projections and 95% credible intervals, respectively. Projections were obtained using the model fitted to data up to day 110.

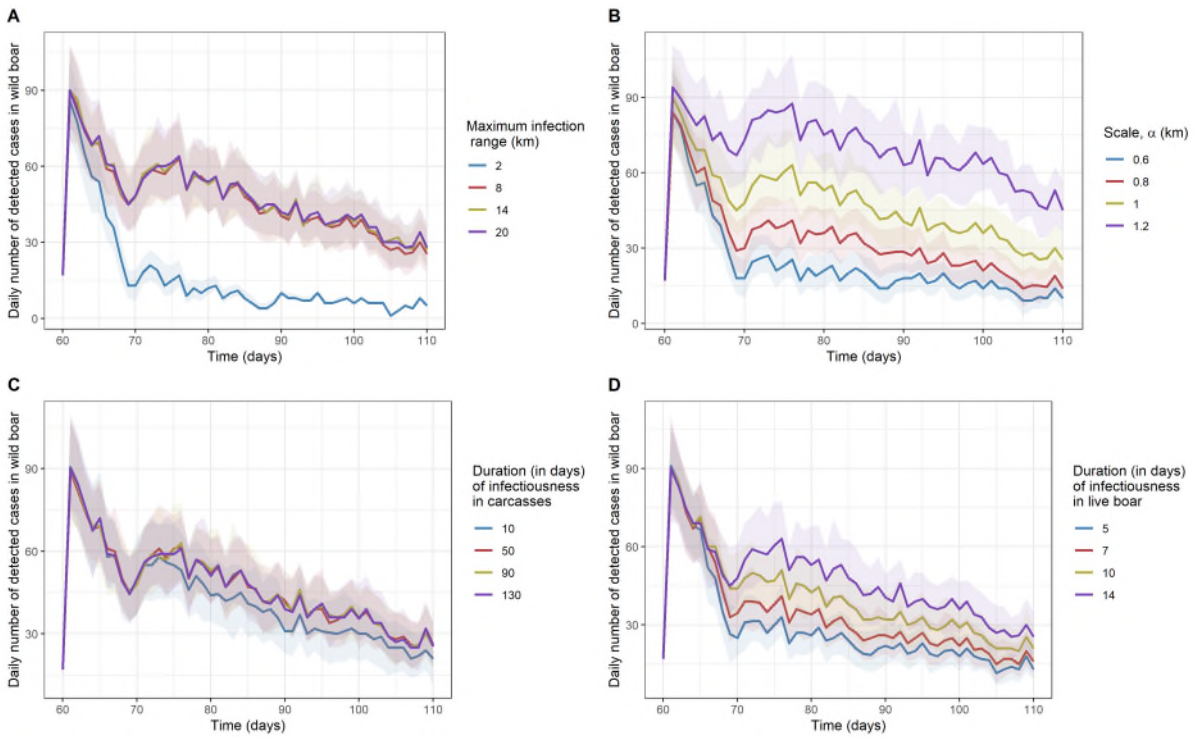

Figure 55: Sensitivity of the daily number of detected infected wild boar (from day 60 to day 110) to **A**: the maximum infection range (values: 2 km, 8 km, 14 km, 20 km); **B**: the scale parameter α of the dispersal kernel (values: 0.6 km, 0.8 km, 1 km, 1.2 km); **C**: the duration of infectiousness in carcasses (values: 10 days, 50 days, 90 days, 130 days); and **D**: the duration of infectiousness in live boar (values: 5 days, 7 days, 10 days, 14 days). Trajectories are medians computed from 100 stochastic repetitions of the model. Shaded regions are corresponding 95% credible intervals. Simulations corresponding to baseline parameter values (maximum infection range = 8 km, α = 1 km, duration of infectiousness in carcasses = 90 days; and duration of infectiousness in live boar = 14 days) are the same across panels.